NUREG/CR-4079
LA-10307-MS

Los Alamos National Laboratory is operated by the University of California for the United States Department of Energy under contract W-7405-ENG-36

Analytic Studies Pertaining to Steam Generator Tube Rupture Accidents

Los Alamos National Laboratory
Los Alamos, New Mexico 87545

8504060372 850430
PDR NUREG
CR-4079 R PDR

NOTICE

This report was prepared as an account of work sponsored by an agency of the United States Government. Neither the United States Government nor any agency thereof, or any of their employees, makes any warranty, expressed or implied, or assumes any legal liability or responsibility for any third party's use, or the results of such use, of any information, apparatus, product or process disclosed in this report, or represents that its use by such third party would not infringe privately owned rights.

NUREG/CR-4079
LA-10307-MS

R4

Analytic Studies Pertaining to Steam Generator Tube Rupture Accidents

B. A. Kashiwa
R. C. Mjolsness

Manuscript submitted: December 1984
Date published: March 1985

Prepared for
Division of Accident Evaluation
Office of Nuclear Regulatory Research
US Nuclear Regulatory Commission
Washington, DC 20555

NRC FIN No. A7247

Los Alamos National Laboratory
Los Alamos, New Mexico 87545

CONTENTS

ANALYTIC STUDIES PERTAINING TO STEAM GENERATOR TUBE RUPTURE ACCIDENTS

by

B. A. Kashiwa and R. C. Mjolsness

ABSTRACT

A study of the thermal-hydraulic phenomena of possible steam generator tube rupture (SGTR) accidents leads to the conclusions that (1) flashing will not occur upstream of the tube rupture, so that the flow will be resistance limited rather than choked, (2) there is considerable potential for discharging the primary fluid in the form of micron-sized droplets, particularly when the fluid discharges into a vapor cavity surrounding the tube rupture, and (3) that the surrounding of the rupture site by water rather than vapor may be a means for preventing the formation of micron-sized droplets. The presence or absence of micron-sized droplets is considered to be a key issue for the damage assessment of SGTR accidents because they are currently thought to be the most likely route for radioactive iodine to be released to the atmosphere.

I. INTRODUCTION

In the production of electricity using the energy from a pressurized water nuclear reactor (PWR), a steam generator resembling a tube-and-shell heat exchanger must be used. This is because the water needed to transport the heat energy away from the nuclear fuel can contain impurities that are radioactive. Safe use of nuclear energy as a heat source for power generation requires that separate fluid circulation circuits be maintained for removal of heat from the reactor core and for steam passing through turbines powering electrical generators. These two circuits can only be allowed communication by way of heat exchange in the steam generator. If a rupture occurs in a tube inside the steam generator, mixing of the reactor coolant (primary) water with the steam generator (secondary) water will result. Thus a systematic series of investigations, both

theoretical and experimental, is needed to study the steam generator tube rupture (SGTR) problem.

The purpose of this report is to present the results of a set of theoretical investigations into the thermo-hydraulic related facets of SGTR events. There has been some prior work* directed at the same goal,[9] in addition to one study in which the complicated non-equilibrium chemical reactions associated with radionuclide transport have been studied theoretically.[39] Here attention is restricted to thermodynamic, heat transfer, and fluid dynamic concerns; the results extend those of earlier works and provide new insights into the potential consequences of SGTR accidents.

First, it is important to understand the possible sequence of events in a SGTR accident, beginning with the tube rupture and ending with temporary shutdown of the plant. Figure 1 is a schematic of a typical PWR plant showing only those components most relevant to the SGTR accident sequence. The primary circuit consists of the reactor itself and at least two coolant loops as shown in Fig.1-1. Each primary coolant loop transfers heat to the secondary circuit through a steam generator. Rupture of a primary circuit tube in the steam generator provides a pathway for radionuclide release to the atmosphere either through the atmospheric relief valves (ARV "A" or ARV "B") or through the turbine-condenser system. The pressurizer is provided to maintain the primary circuit pressure of 150 bar. High-pressure injection (HPI) of cold water is provided for core cooling under emergency loss-of-coolant accident conditions.

In the event of a SGTR, contaminated primary water enters the secondary circuit and, if concentration is sufficient, radiation monitors will signal an alarm. If the rupture is large enough, however, the flow rate of primary fluid can be large enough to cause the pressurizer to empty rapidly, causing another alarm to signal. If the pressurizer is unable to prevent the primary circuit pressure from dropping below a specified value (typically about 130 bar), then the system automatically enters an emergency response sequence. In this the following four actions occur essentially simultaneously

1. Control rods are actuated to terminate the production of thermal energy in the core (called reactor scram or reactor trip).
2. The main feed-water (MFW) pumps on the steam generators are stopped.
3. Auxiliary feed-water pumping for the steam generators is initiated.

*In this report references are numbered in alphabetical order (see reference list).

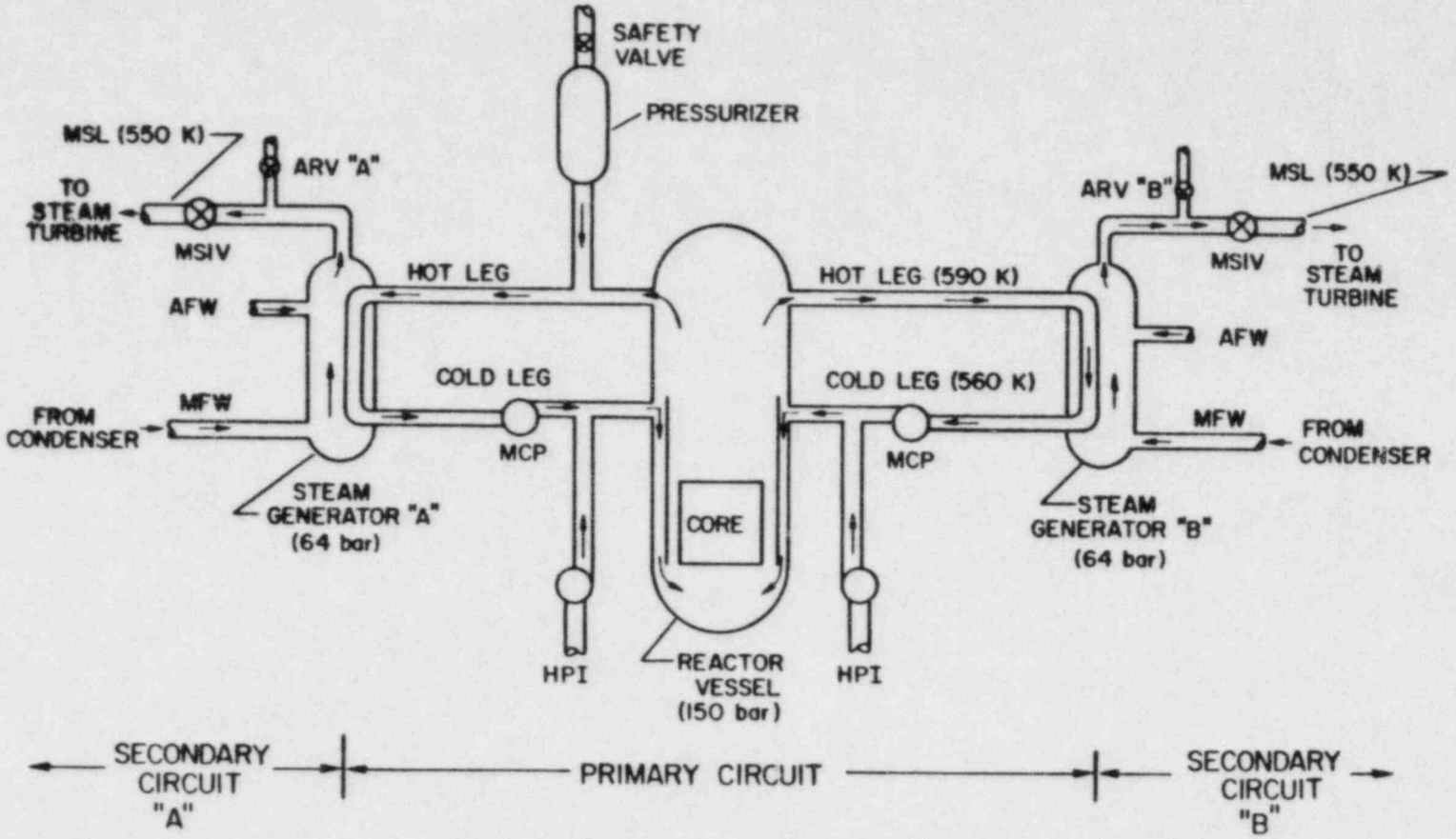

Fig. 1-1. Schematic of a typical pressurized water reactor plant showing parts relevant to SGTR accidents. Abbreviations are: MSL-main steam line, MSIV-main steam line isolation valve, ARV-atomospheric relief valve, MFW-main feedwater, AFW-auxiliary feedwater, MCP-main coolant pump, and HPI-high pressure injection.

4. The flow of steam to the turbines is terminated by closing either the main steam line isolation valves (MSIV's) or a turbine stop valve.

If the reactor vessel pressure continues to drop and a pressure of about 110 bar is reached, HPI injection is automatically initiated. About one minute after initiation of HPI injection, the main coolant pumps (MCP's) are turned off. The action of closing the MSIV's or the turbine stop valve causes the steam generator pressure to rise quickly. In the more severe accidents, the condensing system is not available to accommodate excess steam. Therefore, in this case, when the steam generator pressure reaches about 70 bar, the atmospheric relief valve (or valves) acts to relieve the excess pressure and maintain a pressure of about 70 bar. The reactor trip causes heat production in the core to stop almost instantly, except for decay heat. Thus the primary coolant temperature drops almost immediately to a temperature of about 560 K, roughly the saturation temperature at 70 bar. The primary pressure remains at a level of from 85 to 145 bar depending on the HPI capacity and HPI dead-head pressure. This means that 560 K primary fluid is passed into the 70 bar steam generator vessel at a rate determined by the primary system pressure; this pressure may vary widely depending on the detailed nature of any particular set of accident conditions and specific plant design.

At this stage, leakage would continue indefinitely unless the operator takes action to depressurize the primary circuit. In typical safety analysis studies one assumes that the rising liquid level in the damaged steam generator alerts the operator to the nature of the system problem. The proper action is to open the ARV's nearest the intact steam generator while closing down HPI flow and shutting down the pressurizer heaters. Because the intact steam generators automatically maintain a fixed water level, cool water will be introduced to them via auxiliary feed water pumping. This sets up a natural circulation in the primary loop and a way of cooling it down. Eventually a primary pressure of 70 bar or less is obtained and flow from the tube rupture is either terminated or reversed. A typical elapsed time for this entire set of events is about 30 min.

During this sequence the possibility of introducing radioactive materials into the atmosphere arises when the damaged steam generator ARV opens in response to the 70 bar pressure limitation. System calculations show that the ARV for the damaged steam generator begins to open and close soon after the primary coolant temperature drops to about 560 K.[13-15,18]

This accident response sequence is considered representative of only the principal features of a typical set of automatic emergency actions. Operator ac-

tion and deviations in plant design from the typical system described cause differences in the detailed nature of the potential accident. The purpose of the foregoing description is only to introduce the basic hardware and terminology needed for understanding the analysis contained in this report. There are a number of possible multiple accidents of concern, two of which are relevant to this report. One is SGTR with loss-of-feedwater (SGTR/LOFW) and another is SGTR with a stuck-open-safety valve (SGTR/SOSV). When these events are combined, the damaged steam generator is boiled dry, so that its internal environment is essentially pure steam.[34] In the single-event SGTR, the steam generator fills with liquid because of MSIV closure. Hence the thermo-hydraulic nature of single versus multiple-event accidents can be vastly different, a point to be examined in this report.

It is clear from the sequence described that the system conditions giving rise to the potential for radioactivity release during the approximately 30 minute transient can be highly variable. The reactor vessel pressure drops continuously and the steam generator pressure rises until it reaches a maximum value. This means that the flow rate of primary fluid into the secondary loop varies continuously. Soon after the reactor scram the temperature of the primary water arriving at the steam generator begins to drop. This means that the heat transfer rate and even the direction of heat exchange in the steam generator also vary throughout the 30 minute transient. A variety of computational system response studies on most of the different PWR plant configurations have been performed.[13-15,18,34] Results of these studies provide the conceptual starting point for the more detailed studies contained in this report.

The principal radioactive species of concern in SGTR accidents is radioactive iodine, which is present in the primary coolant at varying concentrations.[39] The exact chemical forms of the released iodine and their equilibrium chemical and thermodynamic properties under PWR conditions are the subject of other studies.* Of particular concern is the manner in which the dissolved radioiodine in the primary coolant partitions itself between phases of the two-phase mixture resulting from depressurization of the primary fluid. The current knowledge of radioiodine behavior under these circumstances is very limited. About all that can be said is that the so-called partition coefficient, defined as the ratio of radioiodine concentration in the water to that in the steam at a given saturation

*Information provided by S. D. Clinton, Oak Ridge National Laboratory, July 1984.

condition, can vary widely depending on the pH of the water.[39] An understanding of the physical chemistry of the system appears to be an objective attainable only in the future. Therefore at this time, experiments designed to give engineering estimates of the partition coefficient are under way to provide an interim understanding of radioiodine behavior in steam-water mixtures.*

The present SGTR transient studies are aimed at better understanding the thermo-hydraulic facets of potential radioiodine release. The approach is to trace the path of the discharged primary fluid during its excursion from the rupture site into the steam generator cavity and eventually to the environment. The amount of radioiodine release will then be a function of initial concentration in the primary fluid and the partition coefficient. In this study it is assumed that these factors are or will be available from other investigations.

The travel of the discharged primary fluid can be divided into four segments

1. Flow from the primary circuit up to and through rupture site.
2. Flow of the primary fluid from just downstream of the rupture into the neighboring region of the steam generator cavity.
3. Upward flow of the discharged fluid and subsequent mixing with the secondary steam-water mixture through the tube bundle and support structure to the top of the tubes.
4. Flow through the separator and dryer region of the steam generator, and release to the atmosphere through the ARV.

Figure 1-2 is a schematic of the U-tube type of steam generators used in PWR plants. This figure provides an idea of the locations of the four flow regions.

Shortly after the rupture occurs, primary fluid will flow through the broken tube from both the inlet and outlet plenums of the steam generator because of the pressure difference between the primary and secondary circuits. In the initial portion of the transient, the primary fluid arriving at the rupture may be sufficiently superheated with respect to the saturation temperature at the secondary pressure to allow violent flashing to occur at the rupture site. Prior studies[2,12] have concluded that if this is the case then droplets of primary fluid on the order of 10^{-4} cm in size could be formed. Furthermore it has been suggested that if the partition coefficient is large, the presence of micron-sized droplets may be a very important release mechanism for radioactive iodine to the atmosphere.[39] This is because micron-sized droplets are not well removed from the steam in the separator and dryer region of the steam generator.

*Information provided by S. D. Clinton, Oak Ridge National Laboratory, July 1984.

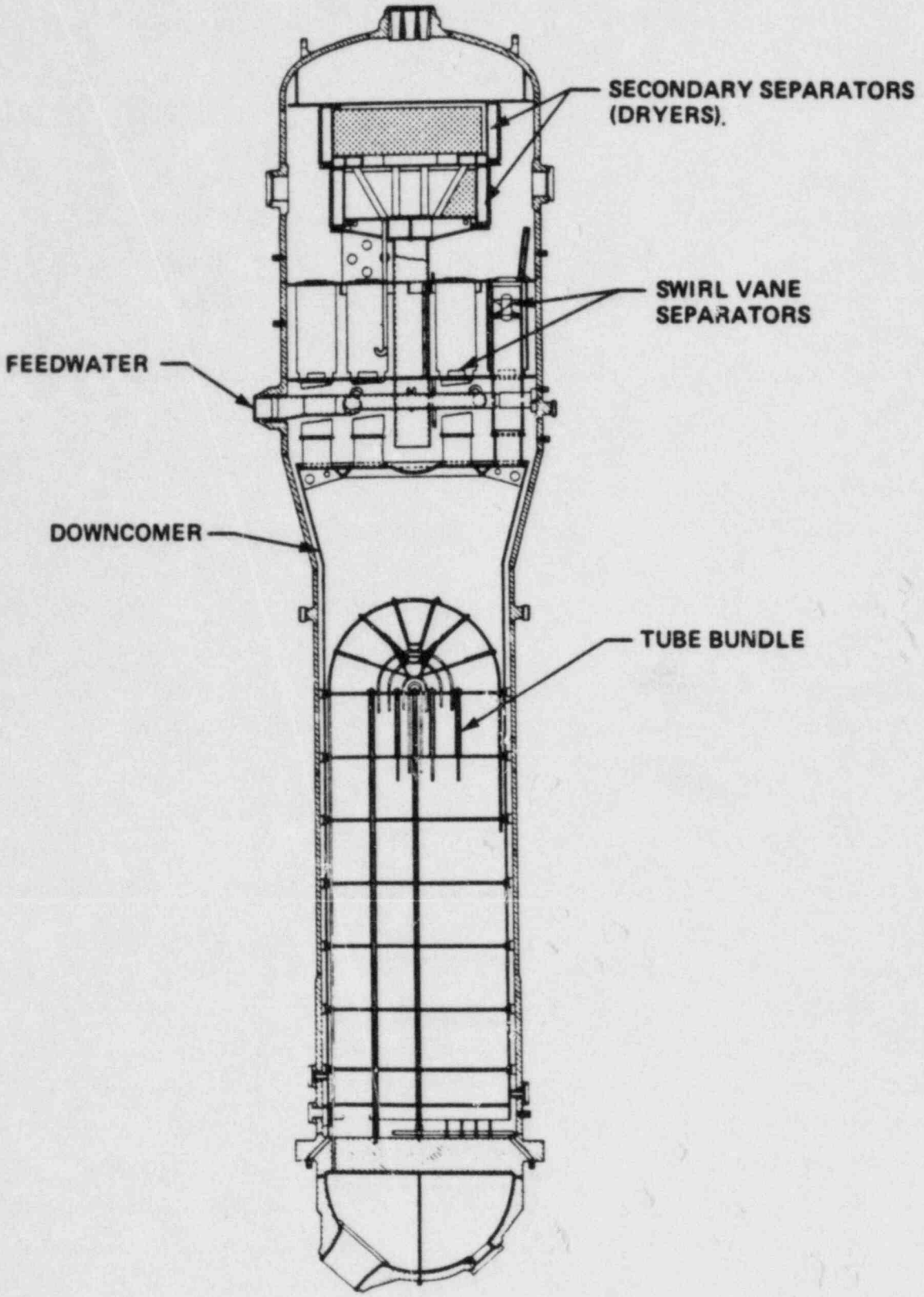

Fig. 1-2. Schematic of a typical U-Tube steam generator. Courtesy of Westinghouse Electric Company

The studies reported here are divided according to the four flow regions just listed. In the next section a detailed study of the primary discharge flow rate is presented. In this, careful examination is made of the physical mechanisms determining the flow rate as a function of conditions in the hot and cold side plenums, heat transfer to the broken tube, and position of the rupture. To explore the role of the various mechanisms a variety of sample calculations are performed. We conclude that flashing does not occur upstream of the tube rupture. In Sec. III the question of droplet formation or nonformation is addressed. The results of Sec. II provide the needed set of boundary conditions to examine the relative role of a number of mechanisms by which droplets may be formed. A series of sample calculations is again performed to illustrate possible effects. In Sec. IV the transport of the primary-secondary, two-phase mixture through the tube bundle is examined. Methods to determine the general nature of the distribution of discharged primary fluid approaching the dryer-separator region are given. Since the separation efficiency of these devices is considered well known, analysis of region four is not included in this study. Thus the parts of the radioiodine flow path requiring added illumination have been pointed out and recommendations have been made for their quantitative analysis. Section V highlights the relevance of the current study to others presently under way. Section VI lists the major conclusions of this study.

II. FLOW OF THE PRIMARY FLUID TO THE RUPTURE SITE

This section discusses the nature of the flow of primary coolant from both the hot and cold side steam generator (SG) plenums, through the broken tube, up to and through the rupture site. There are two principal concerns in this part of the problem. The first is to determine the discharge rate for primary coolant passing through the rupture as a function of conditions in the hot and cold side SG plenums and the secondary environment into which the discharge flows. The second problem is to determine the amount of flashing that may have occurred in the discharged coolant, either upstream, at, or just outside the rupture. Establishing the most likely state of the primary discharge just outside the rupture is an important first step in SGTR analysis. The hydrodynamic state at this position serves as a boundary condition for analysis of subsequent flow regions; it also may be of considerable significance in determining the hazard potential in the SGTR event.

In calculating the discharge flow rate, one must give proper attention to each of two possible mechanisms by which the flow rate can be determined. One mechanism is the depressed sound speed that is characteristic of gas-liquid mixtures and gives rise to the phenomenon of choked flow for such mixtures. The other mechanism is flow resistance, which results in a fluid flow rate limited by pipe friction and the impedances of inlets, outlets, bends, constrictions, etc.

The principal conclusions of the section are that there is no upstream flashing in the initial stages of an SGTR accident, and probably not in any stages of the accident, and that there is a potentially enhanced flow of primary water into the secondary circuit because the flow in the ruptured tube is not choked. In the following we describe the thermo-hydrodynamic conditions encountered in the ruptured tube, explain our mode of analysis of these conditions, and present our results.

A. Flow-Limiting Mechanisms

Critical two-phase flow is a well-known phenomenon in reactor safety analysis. Just as for critical flow in single-phase gas dynamics, critical two-phase flow occurs when the flow speed u reaches the mixture sound speed c. For internal flows, as for example in a converging-diverging nozzle, this means that changes in pressure downstream of the point where u = c cannot affect the flow speed. In systems for which critical two-phase flow is the flow rate determining mechanism, an estimate of the flow rate can be obtained with the homogeneous equilibrium model (HEM). For a vessel of compressed liquid of density ρ_o, at pressure p_o and temperature T_o, the HEM gives the critical mass flow rate G_c as

$$G_c = [x\rho_{v,t} + (1 - x)\rho_{\ell,t}]\left(\frac{2(p_o - p_t)}{\rho_o}\right)^{1/2} . \qquad (2\text{-}1)$$

Here x, $\rho_{v,t}$, $\rho_{\ell,t}$ are the quality (mass of vapor per unit mixture mass), vapor density and liquid density corresponding to the pressure p_t that maximizes the function of Eq. (2-1) subject to the condition that the mixture entropy equals the initial entropy $s_o(p_o, T_o)$. Thus the HEM assumes depressurization along an isentrope, thermodynamic (temperature) equilibrium between the vapor and liquid, and equal velocity of the vapor and liquid. For circumstances where there is sufficient time for the flow to reach both thermal equilibrium and homogeneity in velocity, the HEM gives accurate results. In cases such as discharge through an orifice, there may not be time for homogeneous equilibrium conditions to be

achieved. For these cases empirical correlations exist, which are usually sufficient to account for the effects of nonequilibrium and non-equal velocity.

If two-phase flow occurs in the ruptured tube early in the accident, the resulting flow will surely be critical, due to the large pressure difference between the primary and secondary circuits. Later the pressure difference is much smaller and if two-phase flow occurs then, it will be a resistance-limited flow whose resistance is altered by the two-phase conditions.[19]

To specify a general (one-phase or two-phase) resistance-limited flow consider the steady flow of a pure liquid from a vessel at pressure p_o through a pipe of length L, diameter D, and friction coefficient f. If the entrance and exit loss coefficients are given by K_1 and K_2 respectively, then the flow speed u is determined by the Darcy-Weisback equation

$$(p_o - p_a) = \left(K_1 + f\,\frac{L}{D} + K_2\right)\frac{1}{2}\,\rho_o u^2 \qquad (2\text{-}2)$$

where ρ_o is the fluid density and p_a is the pressure outside the pipe. In the case of incompressible one-phase flow, Eq. (2-2) can be used to determine the pressure p(Z) as a function of distance along the pipe Z, once the steady flow speed in the pipe u is determined. To do this one uses $\Delta p_i = K_i \frac{1}{2}\,\rho_o u^2$ at the entrance (i = 1) and exit (i = 2) and $\Delta p_Z = f\,\frac{Z}{D}\,\frac{1}{2}\,\rho_o u^2$ in between. The result of this is a pressure profile showing a discontinuous change in pressure at the entrance and exit (the so-called point losses) and a linear change in pressure for $0 < Z < L$.

Equation (2-2) also describes resistance-limited two-phase flow, but the impedances K_1, K_2, and f have somewhat altered values, due to two-phase flow effects. In addition ρ_o is not strictly constant in the two-phase case but, because the flow is subsonic, it is not highly variable once the mixture flow appears. Of course, in the case of critical flow an analog of Eq. (2-2) also holds, but the exit pressure p_e is not the ambient pressure (the equation serves to determine p_e) and there is a further pressure drop to p_a outside the tube in a two-phase jet.

The foregoing discussion has indicated that the applicability of Eq. (2-1) versus that of Eq. (2-2) in determining the flow speed depends on two things. Both depend on the unknown geometry of the rupture. In order to have two-phase flow, the series of flow impedances must be such that a pressure less than the saturation pressure is reached somewhat upstream of the exit, and there must be

sufficient time for nucleation to occur and for bubble formation to succeed in choking the flow. Whereas K_1 and f are known as functions of entrance geometry and pipe roughness respectively, K_2 is undetermined except for ruptures that have already occurred. Therefore, in the following we examine what value of K_2 suffices to prevent the flow from flashing in the tube; we conclude that boiling is limited to regions beyond the exit.

B. Question of Upstream Flashing in SGTR

The fluid flow upstream of the break in SGTR is mildly three-dimensional fairly far upstream, with streamlines having some variation in angle as well as radius, allowing the fluid to adjust to conditions in the immediate vicinity of the break, where the flow is fully three-dimensional and where, in particular, pressure gradients are set up to offset the centrifugal force on a fluid element as it exits the tube. Apart from a rapid transient upon rupture, the flow is essentially time-independent in an average sense, although important turbulent fluctuations persist throughout the tube at all times and, if flashing occurs just outside the rupture, the instantaneous flow field just outside the rupture will be very ragged and variable. We confront the fully three-dimensional flow at the exit only in the crudest sense when, in the concluding paragraphs, we attempt to produce and assess simplistic models for the exit impedance K_2 produced by the rupture. However, the mild three-dimensionality and quasistatic behavior of the mean flow upstream of the rupture justify treating this flow as fully one-dimensional. Thus we will continue to use Eq. (2-2) whenever we have impedance limited, one-phase flow up to the rupture. In particular, we will use its local analog,

$$\left(p_o - p(Z)\right) = \left(K_1 + f\,\frac{Z}{D}\right)\frac{1}{2}\,\rho_o u^2 \quad , \tag{2-2a}$$

applied up to the point of rupture to determine the exit impedance K_2 that would suffice to prevent the flow from flashing upstream. The ever-present turbulent fluctuations, with their effects on fluid velocity profiles and fluid resistance, are fully accounted for in Eqs. (2-2) and (2-2a) by the empirical values of K_1, K_2 and f.

We thus treat the flows in the ruptured tube as stationary, even though there is a slow time-dependence during the course of the hypothetical SGTR accident as pressures and temperatures change (and mostly decrease) in response to the rup-

ture and the corrective system actions taken in consequence of the rupture. We will show here that it is overwhelmingly probable that there is no upstream flashing in the initial phase of the SGTR accident. Whether upstream flashing will occur in later phases of the accident depends on the complex pressure and thermal history of water in the hot and cold leg affected by the rupture. This question can be answered more definitively by the methods of this section, given the pressure-time history and the thermal-time history of the fluids in the hot and the cold legs during the course of the SGTR accident. We do not study the question here since we presently lack the needed time histories.

While we are confident that upstream flashing will not occur in the initial phase of a SGTR accident, we can at present assess the prospects for upstream flashing during the later stages of the accident only very crudely, as follows. The possibility for upstream flashing arises because the water in the primary circuit, which is subcooled under normal operation of the reactor, contains superheat initially when it exits the tube rupture. We show in this section that the initial superheat is most unlikely to be sufficient to cause upstream flashing. Whether flashing occurs subsequently depends primarily on whether the water in the hot and cold legs first has a substantial decrease in temperature (and thus has little or no superheat at each spatial location as it exits the tube) or in pressure (and thus has substantial superheat over a substantial region of the tube prior to exiting, leading to upstream flashing). Previous SGTR simulations[13-15] indicate that the major loss of temperature occurs first. Thus both the loss of superheat and the reduction in the flow driving pressure differential decrease the probability for critical flow conditions at the exit; the chance of upstream flashing is reduced, while the likelihood of driving the flow to critical conditions is also reduced, even if the flow does flash inside the tube. Thus it is certainly reasonable to presume that the flow will be resistance limited at all stages of the accident, but the whole matter needs to be settled by calculations.

We now review the arguments leading to the conclusion that in the initial phase of the SGTR accidents there is no upstream flashing. We first compute the exit point impedance K_2 necessary to keep the exit pressure p_e at or above the saturation pressure p_s at the exit mixed mean fluid temperature T_e, an exit pressure sufficient to suppress strong boiling upstream of the rupture and thus eliminate upstream flashing.[41,42] We then estimate very crudely the exit impedance K_2 that a tube rupture can be expected to produce. We find that the estimated K_2 is substantially more than needed to suppress upstream flashing.

The critical exit impedance K_2 is set by the flow of water from the hot leg. We analyze this flow as a one-dimensional flow, using Eqs. (2-2) and

$$p(Z_e) = p_s(T_e) = p_e \quad . \tag{2-3}$$

These conditions suffice to prevent upstream flashing, and we inquire what value of K_2 is needed to enforce them. By supplementing the previous equations with the exit (pre-point resistance) pressure flow conditions

$$p_o - p_e = \left(K_1 + f\,\frac{Z}{D}\right)\left(\frac{1}{2}\,\rho_o u^2\right) \quad , \tag{2-4}$$

where Z now denotes the tube distance from the hot leg to the rupture, we obtain the required value of K_2, namely

$$K_2 = \left(K_1 + f\,\frac{Z}{D}\right)\left(\frac{p_s(T_e) - p_a}{p_o - p_s(T_e)}\right) \quad . \tag{2-5}$$

The first factor in Eq. (2-5) increases with distance Z to the rupture while the second factor decreases with Z (since $p_o > p_s > p_a$, $\frac{dp_s}{dT} > 0$, and $\frac{dT_e}{dZ} < 0$). In general, then, there will be a Z_m for which the needed K_2 is maximal. For typical light water reactor conditions Z_m occurs within the existing tube length and is used to set the required value of K_2 that suffices to prevent upstream flashing.

Although Eq. (2-5) is formally an extremely simple equation, there are some complications and uncertainties in applying it under conditions typical of a SGTR accident in a commonly constructed light water reactor. We may take $K_1 = 0.5$ to adequate accuracy. Similarly, for the large Reynolds number (and, hence, turbulent flows) typical of tube flow under either normal or SGTR operating conditions we may take $f = 0.013$ without serious error. While the unruptured tube diameter D is, of course, known, Z can only be determined immediately to about 2 cm, which is certainly adequate in a long tube. However, significant uncertainties can arise from the pressures. Only initially do we know the hot leg pressure p_o and the pressure in the secondary system p_a without an extensive, realistic simulation of the SGTR accident. This is the essential rationale for confining the

definite conclusions of this report to the initial phase of the accident. Finally, p_s is subject to uncertainty at all times. This saturation pressure can be evaluated by interpolation in the Steam Tables when T_e is known, but T_e is the result of an enormously complex heat transfer process. Here we can only attempt an approximate treatment of the heat transfer and will have to accept uncertainty in the final determination of T_e and p_s.

We outline the convective-conductive processes of heat transfer following a SGTR, enumerating the points that complicate the normal sort of heat transfer analysis. The flow in the tube is turbulent but essentially one-dimensional, permitting the possibility of conventional analysis. However, the velocity flow field is not fully developed at the tube entrance, as conventionally assumed, so the temperature drop in the entrance region will not be correctly given by conventional analysis. This, in turn, will introduce error into the final determination of the exit temperature T_e. However, the largest uncertainties are associated with the heat transfer to the wall from the tube entrance to the tube rupture. The appropriate boundary condition for the fluid temperature T_w at the tube wall is

$$k \frac{\partial}{\partial r} T_w + h(T_w - T_s) = 0 \quad , \tag{2-6}$$

where T_s is the fluid temperature in the secondary system outside the tube wall, k is the thermal conductivity, and h is the heat transfer coefficient. This condition involves coefficients k, h, and T_s that vary both with distance Z along the tube and with angle θ around the circumference of the tube. Moreover, the factors will be somewhat different for each tube in the bundle. The variation in k is greater than an order of magnitude but it is the simplest to characterize, since under quasistatic conditions k is adequately characterized as a tabulated function of the local pressure p(Z) and the wall temperature T_w and p(Z) can be adequately given by Eqs. (2-2) and (2-4) (with some residual uncertainty because K_2 cannot be accurately estimated at present). If a value for T_w is postulated, then table look-up and interpolation will yield a value for k. Determination of T_s is much more difficult. Even under normal flow conditions the temperature of the water in the secondary system is known only in a bulk average sense. The temperature $T_s(0)$ is higher by undetermined amounts near the tube walls, where there is a complex, active convective heat transfer process under way. After the tube rupture, the heat transfer process becomes even harder to characterize due

to the strong perturbation of Z and θ dependent (and tube dependent) additional and more vigorous convective processes engendered by the rupture and the possibility of very substantial changes in the already unknown initial value h(0) of the heat transfer coefficient. For example, the more rapid fluid flow after tube rupture leads immediately to an increase in the heat transfer rate along the tube including the vicinity of the tube entrance where the heat transfer process is most vigorous. Should the enhanced heat transfer be sufficient to create a vapor layer over an outside segment of the tube, then after an initial transient the heat transfer in that tube segment will be much reduced, and the water at the tube exit will contain more superheat than would be the case before vapor formation.

Clearly, the rich detail of the actual heat transfer process is only hinted at in the conventional turbulent heat transfer analysis that assumes either a constant wall temperature T_w or a constant heat flux. We will employ the conventional analytical framework, with as much discretion as is possible, to reflect the complex reality of the actual heat transfer process as best we can while still retaining the truly enormous analytical simplification of the conventional analysis, together with the sharp clarity of the conclusions to which this analysis leads.

An additional idealization of the conventional analysis is the assumption of constant fluid transport coefficients k and ν or, equivalently and directly used in the analysis, constant Reynolds number and Prandtl number. We have seen just how variable k is under tube rupture conditions. In addition, the Reynolds number varies by a factor of 6 and the Prandtl number by a factor of 2 under these conditions. We again defer precise treatment of the complex reality, since it is more appropriate to an extensive calculational program, and allow for these effects as best we can by a judicious choice of parameters in the conventional analysis.

For definiteness we will assume that the rupture occurs in a tube in average position in the tube bundle of a Westinghouse Steam Generator. We will take reasonable values for the flow resistance and determine the system dimensions and parameters from a description of the Westinghouse Steam Generator.[55] Specifically we take

$f = 0.013$	(tube wall friction factor)
$K_1 = 0.5$	(entrance point resistance)
$D = 1.97$ cm	(tube diameter)
$L = 2200$ cm	(average tube length)
$T_o = 585.5$ K	(hot side plenum temperature)
$T_{final} = 550$ K	(cold side plenum temperature)
$p_o = 153$ bar	(hot side plenum pressure)
$p_{final} = 150$ bar	(cold side plenum pressure)
$p_a = 50$ bar	(secondary pressure)
$\nu = 1.25 \times 10^{-3}$ cm^2 sec^{-1}	(hot side plenum viscosity)
$Pr = 1.02$	(hot side plenum Prandtl number)
$u_o = 427$ cm sec^{-1}	(unruptured downstream flow velocity)

We initially treat the heat transfer as though it were the simple T_w = constant, fully developed velocity profile, constant fluid transport properties problem treated by Sleicher and Tribus.[47] This still permits some reflection of the complex thermal environment through the choice of T_w, the temperature the circulating water would cool to if the tube were infinitely long. This captures the dominant feature of the turbulent transfer process: that for the mixed mean temperature

$$T_m = \frac{\int_o^{D/2} dr\ ru\ T}{\int_o^{D/2} dr\ ru}$$

nearly all the heat is in the lowest eigenmode, and the remaining heat is dumped to the wall within about ten tube diameters of the entrance to the tube. The subsequent heat transfer process is represented by the decay of heat in the lowest eigenmode. The extremely complex thermal environment for the water in the tube, even prior to rupture, may thus be thought of as primarily altering the lowest eigenvalue of the idealized problem, and is treated that way here when we find that the idealized problem leads to unreasonable heat transfer rates.

The Sleicher and Tribus calculations utilize a fully developed velocity profile, employ the Jenkins correction, normalized to air data, for Prandtl number effects, but also utilize an eddy diffusivity that is discontinuous at the edge of the viscous boundary layer and incorrectly approaches zero at the tube axis. In view of the complex relation between this idealized problem and the actual

heat transfer process we will not correct or improve these calculations, but we will need to extrapolate the Sleicher and Tribus eigenvalues to cover the Reynolds numbers of interest to a SGTR accident. Specifically, we introduce the dimensionless temperature

$$\theta = \left(\frac{T_m - T_w}{T_o - T_w} \right) ,$$

retain only the dominant n = 0 contribution to the exact expansions

$$\theta = \sum_{n=0}^{\infty} C_n R_n(r) \exp \left(- \lambda_n^2 \frac{2Z}{RePr\ D} \right) , \tag{2-7}$$

and

$$T_m = T_w + 8(T_o - T_w) \sum_{n=0}^{\infty} A_n \lambda_n^{-2} \exp \left(- \lambda_n^2 \frac{2Z}{RePr\ D} \right) , \tag{2-8}$$

where

$$A_n = - \frac{1}{2} C_n R_n' \left(\frac{D}{2} \right) ,$$

and determine A_o and λ_o^2 from extrapolation of the Sleicher and Tribus[47] graphs to the range of Re and Pr of interest to us as

$$\lambda_o^2 = 4.4 \times 10^{-2} Re^{0.8} Pr^{0.3} \tag{2-9}$$

and

$$A_o = 5.9 \times 10^{-3} Re^{0.8} Pr^{0.3} . \tag{2-10}$$

This introduces some error into the fitting of initial conditions for T_m, due to the extrapolation process. To resolve this, we retain Eq. (2-9) for λ_o^2 and require that 98% of the temperature difference $(T_o - T_w)$ be initially present in the lowest eigenmode for T_m, a property shared by the exact solution.

In applying this formalism to the undisturbed flow before the SGTR we must take T_w = 550 K, because of the efficient heat transfer implied by the Sleicher and Tribus formalism. Using the Westinghouse SG parameters quoted earlier, the

undisturbed Reynolds number $Re_o = 6.7 \times 10^5$ and we represent the mixed mean temperature in the bulk of the tube by

$$T_m = 550 + 35 \exp [- \phi(Z)] \quad , \tag{2-11}$$

where

$$\phi(Z) = \frac{8.8 \times 10^{-2} Z}{Re^{0.2} Pr^{0.7} D} \quad . \tag{2-12}$$

We note that $\phi(2200) = 6.58$ and $\exp [-\phi(2200)] = 0.00139$, which implies that according to this model less than 4% of the excess heat carried by T_m upon entry to the tube is transferred to the secondary circuit in the last half of the tube and only 11% of this heat is transferred in the last 2/3 of the tube. In short, this model implies that virtually all the heat is transferred in the first 1/3 of the 2200 cm (average) length of the tube bundle. This would be a very inefficient way to design a tube bundle and surely cannot be characteristic of the Westinghouse steam generator, which is thought to be a very well-designed system. In the more complex reality, we have seen that the primary effect of the total thermal environment is to alter (and mostly reduce) the lowest eigenvalue λ_o^2, which also becomes a function of Z. This effect is, in principle, measurable, though it has not been so measured for the Westinghouse or other relevant SG design. Thus, in lieu of measurements, we are at present forced to determine the effective eigenvalue by making an assumption of the efficiency of heat transfer performance that would be demanded in a well-engineered system. We make the specific demand that roughly 90% of the available heat energy be transferred to the secondary circuit by the end of the tube at Z = 2200 cm. Since $T_m(2200) = 550$ K, the present model then forces the choice $T_w = 546$ K and a modified λ_o^2 which we display in the equation for the mixed mean temperature, valid over most of the tube length,

$$T_m = 546 + 38.5 \exp \left(- \frac{3.06 \times 10^{-2} Z}{Re^{0.2} Pr^{0.7} D} \right) \quad , \tag{2-13}$$

which we use to analyze the possibility of upstream flashing under SGTR conditions. In principle, the numerical coefficient of Eq. (2-13), which depends on

the total thermal environment but which has been determined from undisturbed conditions prior to tube rupture, should change under SGTR conditions. However, we see no practical way to incorporate this effect at present.

We carry out the evaluation of $p_s(Z)$ and of K_2 from Eq. (2-13) for T(Z) for various assumed points Z of the tube rupture using Westinghouse steam generator parameters and making use of the Steam Tables for saturation and superheat condition. The required exit impedance K_2 is dominated by the flow from the hot side plenum to the site of the tube rupture, which may be specified in Table II-1. It is seen that an exit impedance of $K_2 = 3.0$ is more than sufficient to suppress upstream flashing.

Only the most preliminary estimate can be made for the value of K_2 actually produced by a SGTR event due to the very wide variety of possible tube ruptures, the very small number of actual SGTR occurrences, and the complete absence of measurements of or of detailed three-dimensional hydrodynamic calculations of K_2 for any of the actual SGTR events. However, diagrams of the tube rupture at the R. E. Ginna Nuclear Power Plant exist[35] and will be used as the basis for the very crude models for K_2 that will be presented here.

Two highly idealized models of the exit flow impedance will be discussed. In the first we represent the exit K_2 as the sum of three independent standard point impedances, a tee followed by a contraction followed by an expansion. As

TABLE II-1

EXIT IMPEDANCE VERSUS RUPTURE LOCATION

Downstream Location of Tube Rupture	Exit Impedance Required to Suppress Boiling
Z(cm)	K_2
50	0.8
100	1.0
500	2.2
1000	2.7
1500	2.8
2000	2.8
2100	2.8
2150	2.8

we discuss later, this evaluation will tend to overestimate K_2, since we simply add the individual K's of the point impedances, whereas each of these standard impedance elements requires a complete upstream and also downstream flow pattern to contribute fully to the evaluated K. In the tube rupture context, in which we idealize the rupture as the sum of these three impedance elements, the elements are too close to one another in spatial separation to permit the individual upstream and downstream flow patterns to develop fully.

We estimate the individual point impedances with the aid of the discussion of Streeter.[49] The impedance of the tee may[49] be estimated as

$$K_t = 1.8 \quad .$$

The impedance of the contraction is[49] the product of a point impedance factor K_o (area ratio dependent) and a kinematic factor, the ratio of areas squared, namely

$$K_c = K_o \left(\frac{A_{expanded}}{A_{contracted}} \right)^2 \quad .$$

Numerical evaluation of the areas from an idealized plane projection of the actual Ginna rupture[35] yields

$$A_{contracted} = 0.29 \, A_{expanded} \quad ,$$

and for this area ratio[49]

$$K_o = 0.36 \quad .$$

Altogether, then

$$K_c = 4.0 \quad .$$

Finally, the expansion into the secondary circuit will[49] produce an impedance

$$K_{ex} = 1.0 \quad .$$

We then take for the total exit impedance

$$K_2 = K_t + K_c + K_{ex} \quad , \tag{2-14}$$

or

$$K_2 = 6.8 \quad . \tag{2-14a}$$

For the second model replace the tee of the above model by two elbows in parallel. For an elbow we have[49] an impedance

$$K_e = 1.1 \quad ,$$

and the flow through each leg of the tube sees one elbow as it exits the tube. The total exit impedance provided by this model is therefore

$$K_2 = K_e + K_c + K_{ex} \quad , \tag{2-15}$$

or

$$K_2 = 6.1 \quad . \tag{2-15a}$$

As mentioned previously, these two models tend to overestimate the actual K_2.

Another way to estimate the exit impedance is to view the rupture as an orifice in a pipe. An expression for the equivalent point loss due to an orifice is derived in Appendix A. This is

$$K_2 = \left(\frac{1}{C_o} \cdot \frac{A_1}{A_2} \right)^2$$

where A_1 and A_2 are the pipe and orifice flow areas respectively and C_o is the orifice coefficient. It is rather well known that a sharp-edged orifice has a

coefficient C_o of around 0.61, while a well-rounded orifice has C_o approaching 1.0 (Ref. 4).

The rough opening of a ruptured steam generator tube probably has a C_o closer to that of a sharp-edged orifice. Even with no area restriction, a C_o of 0.61 gives $K_2 = 2.69$; any area restriction at all gives values of K_2 substantially greater. It would require an extensive and costly series of three-dimensional hydrodynamic calculations to determine adequately the extent to which the suppression of upstream and downstream flow patterns associated with the three individual events of the exit of the fluid through the tube rupture (the turning of the fluid, its flow through a contraction and its subsequent reexpansion) lead to a reduction in K_2. For the present, the best estimate we can make of these effects is to say that under nearly all presently contemplated tube rupture conditions we anticipate that

$$K_2 \gtrsim 5.0 \quad . \tag{2-16}$$

Thus, we anticipate that the actual exit impedance K_2 will be roughly twice as large as necessary to suppress upstream flashing. We do not expect upstream flashing to occur for most, or, perhaps, all SGTR accidents.

The preceding considerations are appropriate to the initial stages, occupying the first several (typically 10, usually from 5 to 15) minutes before reactor scram, of an SGTR event, in which upstream flashing would be most likely to occur. After reactor scram there is a rapid drop in primary water temperature to roughly 560 K,[13-15,18,34] but the primary system still is at fairly high pressure. The primary water has much less superheat and is even less likely to undergo upstream flashing than in the initial stages of the event. A very few minutes after reactor scram the secondary system reaches a pressure of 70 bar, roughly the saturation pressure for 560 K water; if no superheat ever occurs then flashing cannot occur anywhere in the vicinity of the rupture site. Thus we do not believe upstream flashing, or choked flow through the tube rupture, will occur at any stage of a SGTR event.

It would be very desirable to confirm fully or disprove our present conclusion that there will be no upstream flashing under SGTR conditions, even though this conclusion arose naturally and very definitively from the present analysis. There is substantial experimental literature available with which to confirm these findings. For example, the data given by Henry and Fauske[19] clearly indi-

cate the approach of the flow rate to that of a pure liquid flowing through a sharp-edged orifice, as the stagnation quality of a two-phase mixture approaches zero. The data of Sozzi and Sutherland[48] show the same trend for flows of water through an orifice. The data of Celata et al.[7,8] for water at high pressures show the same tendency, although the orifice coefficient for their experiments is somewhat in question. For low-pressure water, the data of Brown,[6] Brown and York,[5] Short,[44] and Ostrowski[37] show conclusively that the flow through a sharp-edged orifice is limited by the system impedances and not critical two-phase flow, at the pressure differences approaching those of interest in SGTR.

The relevance of this to SGTR studies is that careful consideration as to exit geometry must be given in calculation of flow rates for estimation of accident effects. Typical nonequilibrium critical flow correlations do not take into account flow losses due to pipe friction or point impedances.[19,38,41,42] The result of this neglect may be to overestimate the flow rate. Alternatively, insufficient spatial resolution of the flow in the rupture vicinity could lead numerical computations of the flow rate to predict a non-existent critical two-phase flow circumstance, the result of which can be a fictitiously low flow rate.

III. FLOW FROM THE RUPTURE SITE INTO THE NEAR RUPTURE REGION

A. Flow Conditions

This section reports a study of the interaction of the fluid discharged from the tube rupture as it first encounters the secondary side environment. In the previous section it was seen that the most likely state of the discharged fluid, immediately at the rupture, is pure liquid. Upon leaving the broken tube, this liquid will be suddenly subjected to the pressure of the secondary side. If its temperature is greater than the saturation temperature at the secondary side pressure, "flashing" (a very sudden and intense boiling) may take place. Before reactor scram, the primary fluid temperature can be as high as about 590 K; shortly after reactor scram this drops to about 562 K. The steam generator pressure is set at about 64 bar under normal operation and rapidly increases to about 71 bar soon after reactor scram (which is accompanied by closure of the main steam line isolation valve).[13,34] Therefore the superheat in the liquid just outside the tube rupture can be as high as 37 K initially (up to about 500 s after the rupture occurs) and around 2 K for the remainder of the accident. Thus the potential for existence of a flashing jet may exist throughout the SGTR transient. Although the 2 K superheat at late times is based on best-estimate calcu-

lations,[13,34] it should be recognized that a small difference in the physical system compared to the computed system could mean that fluid is actually subcooled rather than superheated at late times.

The flashing of a superheated liquid in a jet has been studied in connection with spray atomization [5,6,28,29,37,44] and nonequilibrium critical flow.[7,8] These experimental studies serve as an important basis for advancing the theory of nucleation in the boiling of liquids. Apart from the attractive features of the data from a theoretical standpoint, an important experimental fact has emerged concerning the size of droplets in the spray of a flashing jet. In a variety of studies droplets of a size scale on the order of one micron have been observed in these sprays.[5,6,28,29,37,44] Since the important radioactive material in the primary discharge is expected to be non-volatile, it will tend to remain in solution.[23] This means that droplet transport may be the principal mechanism for migration of the radioactive species. Furthermore it has been shown that micron-sized dispersed solid fragments in a gas accommodate to changes in the gas velocity almost instantly.[11] This means that droplets on a size scale of 10^{-4} cm may not be removed by typical steam generator separators, allowing primary fluid to reach the atmosphere through the ARV. Hence the tiny droplets from a flashing jet may pose the greatest threat in terms of radioactivity release in SGTR accidents.[23]

Since the theoretical evidence points to the possibility of the presence of a 2 K superheat at times greater than about 500 s in a typical SGTR accident,[13,34] the following work will assume this to be the case. It is emphasized, however, that small differences in the actual system configuration (e.g. ARV set-point pressure) or small differences in the actual transient (e.g. level of decay heating) could result in a subcooled liquid jet rather than a superheated liquid jet. In the former circumstance no flashing will occur and the primary fluid will simply mix with the secondary liquid causing the concentration of radioactive material to diminish. In this case the only source of droplets is at the liquid surface in the steam generator, where bubble bursting due to pool boiling can occur, during the periodic depressurization which accompanies ARV operation.[34] The droplet formation and entrainment in this case is the subject of other studies.[3]

In the accident scenarios discussed in Sec. I, the steam generator may or may not fill with liquid during the transient, depending on the type of accident considered. Therefore it is important to consider droplet formation in the

flashing jet in environments of both vapor and liquid. The entire body of knowledge concerning droplet formation in the flashing jet is for the case of a jet discharged into a vapor. The case of a flashing jet discharged into a cool liquid has not yet been studied directly, either experimentally or theoretically. Hence the bulk of the current section is directed toward the former case; the latter circumstance is discussed briefly in Sec. G, but largely left open to future study.

For the purposes of this analysis, the flow conditions at the rupture exit plane can be estimated by the methods of the previous section. By assuming an exit impedance and a wall temperature of 546 K one can easily tabulate the exit velocity and the temperatures of the hot and cold side discharge streams for various rupture locations. Having done this, one must then address the question of how the liquid jet disintegrates under the various forces acting on it.

Immediately upon leaving the tube rupture, the liquid jet is subjected to destabilizing forces at its free surface. The nature of this first class of force is very complicated and can be supposed to be composed of a variety of competing effects.[22] For example, the turbulence in the fluid, shear at the free surface, surface evaporation, and surface tension probably play an important part in determining the destabilizing force. In addition, there may be an internal disruptive force generated by the growth of vapor bubbles at nucleation sites distributed throughout the liquid jet.[12] These nucleation sites may be in the form of cavitating suspended particulates, tiny bubbles of insoluble gas or even cavitating heavy molecules of a heavy compound dissolved in the liquid.

The actual interplay of the foregoing effects is very complex, making it extremely difficult to infer theoretically the resulting jet disintegration. However, the experimental data of Brown and York[5,6] suggest that a special case of homogeneous nucleation occurs in the jet. Brown and York examined the disintegration of a jet of hot water exiting various types of orifices into a room at atmospheric pressure. They carefully measured the superheat needed in the liquid water jet in order to obtain a very fine spray of water droplets (called "jet shattering"). These workers observed the existence of a critical superheat, below which jet shattering did not occur, and determined the critical superheat for various flow speeds. (The critical superheat was reported as a bubble growth rate coefficient and the flow speed reported as a Weber number based on exit velocity and orifice diameter.) The resulting plot of superheat versus flow speed shows that the critical superheat tends to very small values as the flow speed

becomes large. At low speeds Brown and York found critical superheats as high as about 30 K at the lowest flow speed and as low as about 2 K at the highest speed tested.[5,6] In a later study under the same experimental conditions, Ostrowski[37] concluded that nucleation takes place throughout the superheated liquid jet in the form of homogeneous nucleation. This results in the growth of many small bubbles whose unbounded growth eventually lends to jet shattering.

Classical homogeneous nucleation theory predicts a maximum attainable superheat of 166 K for water; a value close to the experimental value of 170 K. In order to place any weight on Ostrowski's conclusion, an explanation is needed as to how the maximum attainable superheat from the classical theory is lowered in the case of flowing experiments. One such explanation is set forth in the following section.

B. Extended Theory of Homogeneous Nucleation

This section provides a rough quantitative examination of the foregoing ideas connected with homogeneous nucleation in an accelerating superheated fluid. It is shown that nucleation is highly likely throughout the liquid jet under typical SGTR discharge conditions, provided that there is almost any amount of superheat in the liquid jet. This means that a flashing jet may occur throughout the extent of a SGTR accident. The arguments leading to this conclusion are based on an extension to the classical theory of homogeneous nucleation.

The classical theory of homogeneous nucleation considers the stability of a small "bubble" in a superheated liquid, produced by the random thermal fluctuations of the molecules in the liquid. These small bubbles remain stable as long as they satisfy the condition on size r

$$r < \frac{2\sigma}{\Delta p_s} \tag{3-1}$$

where σ is the surface tension and Δp_s is the difference between the saturation pressure at the superheated liquid temperature and the pressure in the liquid. Stable bubbles satisfying this size condition are continuously produced and destroyed in the liquid; bubbles violating the size condition are considered unstable, in which case their unbounded growth causes them to be removed from the system. Thus a stationary bubble size distribution is formed, whose character depends on the temperature of the system and on the energy of formation of the bub-

ble. If the temperature is increased, a level is eventually reached where nearly all the bubbles formed are unstable. This is the maximum attainable superheat.[10]

To reconcile the experimental data such as those of Brown and York and lend credence to the conclusion of Ostrowski, one must realize that the classical theory of homogeneous nucleation does not consider the effects of relative motion between the small bubbles (sometimes called "embryos") and the surrounding liquid.[25,43,46] In the case of a jet of liquid formed by ejection through an orifice, a sudden acceleration is experienced by the liquid in passing through the orifice. Any tiny bubbles present in the liquid during the acceleration will undergo a deformation as a result of their motion relative to the liquid. The bubbles will tend to accelerate momentarily to a higher velocity than the liquid, due to their lower mass density and the fact that both materials experience the same pressure gradient. It is this deformation that is expected to cause normally stable bubbles to become unstable, lowering the attainable superheat. In the experimental data cited, the higher the velocity of the liquid jet, the greater the acceleration at the orifice must be. Hence one would expect the attainable superheat or "shattering temperature" to decrease with increasing flow speed, as was found in the experiments.[5,6,37,44]

Some degree of credibility can be attached to these ideas by the following dimensional analysis. Suppose the quantities of importance in determining a "shattering" criterion are the acceleration at the orifice a, the degree of superheat, surface tension σ and the mass associated with a typical nucleation embryo m at the local fluid temperature. The degree of superheat can be expressed as the pressure difference Δp_s. Hence, these are four quantities in the three dimensions mass, length, and time. Therefore one can expect to construct a single non-dimensional group from them. One such grouping is

$$N_s = \frac{\Delta p_s a m}{\sigma^2}$$

where an increase in the value of the "shattering number" N_s implies a greater propensity for shattering. The acceleration a can be estimated, for the purpose of comparison to the experiments, from the pressure drop at the orifice according to

$$a = \frac{\Delta p_e}{\rho_\ell \Delta D_o}$$

where Δp_e is the orifice pressure drop, ρ_ℓ is the liquid density and ΔD_o the change in size of the flow conduit from the pipe to the orifice. ΔD_o is taken to represent the distance over which the acceleration takes place. With this representation of acceleration, a reasonable selection for m must involve the liquid density rather than a gas density. If the virtual mass of a bubble of size r is chosen, then N_s can be written

$$N_s = \frac{\Delta p_s \Delta p_e r^3}{\sigma^2 \Delta D_o} \quad . \tag{3-2}$$

This expression is seen to indicate the proper direction in tendency to produce jet shattering with variations in its constituent quantities. Note that the characteristic size of an embryo r is expected to increase with increasing fluid temperature.

Since Ostrowski defined the shattering temperature as the minimum temperature at which thorough nucleation was observed, one can expect N_s to be a constant under those experimental conditions. The value of that constant will give the shattering criterion. Table III-1 lists the relevant conditions from Ostrowski's experiments, together with N_s at each condition. Since a general expression for r, as a function of fluid properties and temperature, is not available, a constant value of 5×10^{-7} cm has been used. This value corresponds to the equilibrium nucleus size at the maximum attainable superheat of pure water at atmospheric pressure as determined by experiment.[10]

The standard variation in N_s about the mean of 6.31×10^{-10} is 21% of the mean in Table III-1. This is a good degree of constancy considering the subjective nature of the definition of the shattering temperature used by Ostrowski.

At 585 K, the temperature characteristic of the primary fluid in SGTR, the surface tension of water is about a factor of 10 smaller than at the atmospheric saturation temperature. Therefore the superheat needed to reach a value of N_s of 6×10^{-10} is only about 0.1 K.

Thus the question of primary system fluid temperature, at late times in a SGTR accident, may become an important issue, if the actual fluid is subcooled

TABLE III-1

VALUES OF N_s FOR OSTROWSKI'S TEST DATA

D_o (cm)	$\Delta p_s(T_r)$ (bar)	Δp_e (bar)	σ $\frac{\text{dynes}}{\text{m}}$	ΔD_o (cm)	$N_s \times 10^{10}$
0.076	4.38	4.08	49.9	1.43	4.84
0.076	4.32	6.12	50.1	1.43	7.08
0.076	4.00	8.16	50.8	1.43	8.29
0.1041	4.35	4.08	49.9	1.40	4.90
0.1041	3.93	6.12	50.8	1.40	6.20
0.1041	3.63	8.16	51.5	1.40	7.22
0.1349	4.32	4.08	50.2	1.37	4.90
0.1349	3.70	6.12	51.1	1.37	7.91
0.1349	3.04	8.16	52.7	1.37	5.47

Average, $\overline{N_s}$ = 6.31, standard deviation 1.36 (21% of $\overline{N_s}$)

entirely for the greatest share of the transient. If however, the discharge is even slightly superheated, as indicated by best-estimate calculations,[13,34] then flashing may occur throughout the accident. Since both possibilities exist, a systematic study of droplet formation in each case is needed.

When flashing does occur, the shattering process itself must be examined in more detail in order to quantify the resulting droplet size. A number of experimental results for flashing liquid jets exist in addition to those already cited, each of which contributes to formation of the conclusion that the flashing liquid jet has a special structure (in contrast to single-phase jets). That structure is characterized as follows.[5-8,17,26,28,33,37,44] A solid column of liquid, roughly the size and shape of the flow opening, emerges from the flow opening and persists for some distance. Because of the high sound speed in the liquid (compared to a two-phase signal propagation speed) the pressure in the liquid column rapidly adjusts to the ambient value. This pressure is necessarily one that is associated with an equilibrium temperature lower than the temperature of the liquid column; therefore the liquid very rapidly becomes superheated. The distance over which the superheated liquid column can persist depends on the mechanism causing the disruption of the liquid column.

As already mentioned, if the sudden depressurization is accompanied by a strong acceleration, homogeneous nucleation can take place. When this is the case, the growth of many bubbles in the liquid jet eventually causes its disruption.[37] If this is not the case, then the ever-present aerodynamic forces acting at the liquid-vapor interface cause an instability of the Kelvin-Helmholtz type to rupture the liquid jet eventually.[22] Ostrowski observed that when the latter mechanism was responsible for jet breakup, the time required for the disruptive process to take place was far greater than when homogeneous nucleation occurred.[37] Ostrowski also observed that when homogeneous nucleation did occur, the number of bubbles generated at a given flow speed increased with the degree of superheat. For values of superheat lying between the minimum needed to produce any nucleation and that which was defined as the shattering superheat, the central core remained sufficiently visible to allow measurement of its length.[37]

Hence, according to the observations of Brown and York,[5] York,[6] Short,[44] and Ostrowski,[37] when no nucleation occurs, the breakup of the superheated jet resembles that of a cold liquid jet, and presumably happens as a result of aerodynamic instabilities. However when nucleation does occur, the growth of bubbles in the liquid either completely or partially ruptures the liquid column, depending on the number of bubbles created. In either case a great volume of vapor is generated whose lateral motion causes liquid fragments to deviate from their predominantly axial pathlines. Hence the cross-sectional area of the jet widens rapidly giving the flashing two-phase jet a much wider divergence angle than its single-phase counterpart. Celata, et al.[7,8] observed that the jet angle of flashing water jets increased with the degree of superheat in the jet.

The jet structure just described is shown schematically in Fig. 3-1. In actual observation of flashing jets, one cannot always observe a liquid column near the flow aperture because it can be obscured by spray thrown upstream from the initial breakup point. Also, the low vapor volume fraction core is not usually visible because of the spray; its detection may require use of a pressure probe[7,8] or an x-radiographic technique.[17] However, Ostrowski[37] was able to view the core photographically and defined the shattering temperature as the temperature at which the superheat was sufficient to cause such thorough nucleation in the liquid column that the core was essentially of zero length. Ostrowski also observed a significant effect of roughness on the shattering temperature, with increasing roughness causing a decrease in the shattering temperature. This feature of the behavior is in agreement with the idea that sudden acceleration has

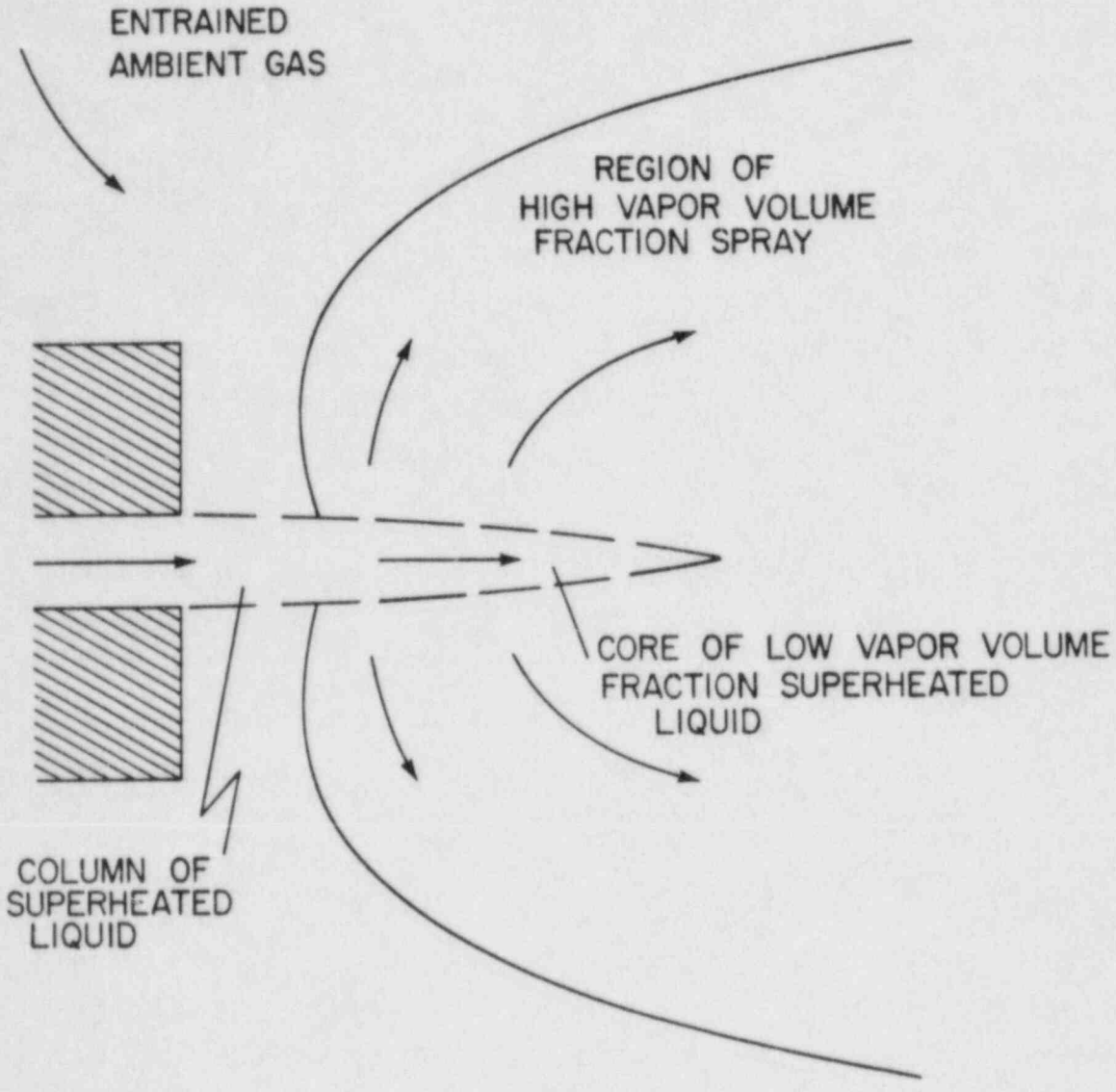

Fig. 3-1. Schematic of a steam-water jet.

the effect of lowering the maximum attainable superheat in a metastable liquid, since the effects of acceleration should be augmented for a rough orifice.

There are two other significant features of the flashing jet data relevant to the present study. The first is the general observation that at a temperature slightly lower than the shattering temperature at a given velocity, an intermittency between a non-flashing and an explosively flashing (shattering) behavior persists.[6,37,44] The second is that at temperatures well below the shattering temperature, but still high enough to create a superheated liquid column, the jet breakup appears to be purely hydrodynamic in nature. That is to say, nucleation does not occur. The consequences of the intermittency for SGTR may be the following. The intermittent flashing jet may well be accompanied by an intermittent thrust causing a fluid-structure interaction to develop. This interaction would be manifested as a sort of pipe-whip. If the foregoing acceleration-influenced nucleation hypothesis is correct, this pipe-whip (or vibration) may cause a further decrease in the attainable superheat, making flashing even more predominant.

The consequences of the non-flashing jet for SGTR accidents are that the droplets formed by aerodynamic atomization may be significantly different in size from those formed by a flashing jet. Since the possibility of both a flashing jet and a non-flashing jet exists in SGTR, a systematic study of droplet formation is needed. The next task is to examine the process of droplet formation in a variety of circumstances. Immediately upon exit from the tube, the jet undergoes primary fragmentation due to surface instabilities excited by the roughness of the exit. There are essentially three mechanisms by which the primary fragments can be reduced to a spray of droplets. They are aerodynamic atomization,[22] boiling breakup,[12] and collisional fragmentation.[53] In the case of no nucleation, aerodynamic atomization will take place. Although the details of aerodynamic atomization are quite complicated, there exists a large body of experimental data, which is useful for performing a scoping analysis. Such an analysis is performed in the following section. When nucleation does take place, then "boiling breakup" will occur. Boiling breakup is the process of liquid fragmentation resulting from the growth of a bubble in the interior of the liquid. An analysis of this process and the resulting droplet size scale are contained in Sec. III-D.

Collisional fragmentation is the atomization mechanism arising from the impact of fluid fragments with one another or with surrounding structure. An analysis of this mechanism of droplet formation is given in Sec. III-E.

C. Aerodynamic Atomization

Aerodynamic atomization is of industrial importance in many areas; for example, liquid fuel combustion, spray drying and dispersion of pesticides all require the reduction of a liquid jet to a fine spray. Because of this, a great deal of experimental and theoretical research has been focused on the subject over the past century. This section cannot approach a complete review of the relevant knowledge because of the massive amount of the available material. Therefore only essential and relevant data will be presented and discussed in relation to the current problem of SGTR.

Aerodynamic atomization is the disintegration process by which a balance is approached between the cohesive force of surface tension and the disruptive force due to shearing at the droplet surface created by motion of the droplet relative to its surrounding fluid.[22] If the medium surrounding the droplet is a gas, one may express the force balance using the droplet in a gas. Then one may express the force balance using a droplet Weber number N_d given by

$$N_d = \frac{\rho_g u_r^2 d}{\sigma}$$

where ρ_g is the surrounding gas density, u_r is the local droplet velocity relative to the local gas velocity, d is the droplet size scale and σ is the surface tension at the liquid-gas interface. Experiments have shown that there is a critical value of N_d called the critical Weber number N_c, such that for $N_d > N_c$ the droplet will undergo a deformation that will eventually cause the droplet to fragment.[22] Thus

$$N_d < N_c \tag{3-3}$$

is called the Weber number criterion for droplet stability. For $N_d < N_c$ the droplet may deform and even oscillate but it will not rupture.[22] Experiments and theory both have shown that the value of N_c depends on the viscosity of the deforming droplet and the acceleration of the droplet relative to the gas.[20,21] Typically N_c increases with increasing viscosity and decreases with increasing acceleration.

Of particular relevance to this study is the rate at which the condition $N_d < N_c$ is approached. This is because the disintegrating jet can typically

travel only a very short distance before impacting the outer wall of another tube neighboring the ruptured tube. The extent of this distance is about two tube diameters. At an exit velocity of 5×10^3 cm/s the approximate, typical transit time from rupture exit to impact is 8×10^{-4} s. Thus any atomization process other than splashing on adjacent tubes must act in less than a millisecond, or else splashing itself may be the important breakup process.

Whereas aerodynamic atomization has been studied extensively, most of the detailed experimental work has been performed with very smooth-walled nozzles or smooth-walled orifices. When a steam generator tube ruptures, the resulting flow opening has a surface of fractured metal, which is rough compared to a finely machined orifice. It is well known that a non-flashing liquid jet issuing from a smooth opening can travel many hundreds of jet diameters before disintegration.[33] It is perhaps less well known, however, that a liquid jet issuing at the same speed from a very rough aperture will disintegrate essentially immediately.[37] Since there is not a great deal of experimental data for rough-aperture discharges, a model of aerodynamic atomization for this circumstance is developed here.

Development of the model begins with the assumption of an initial jet breakup, very close to the flow opening, due to the roughness of the opening. The scale of the liquid fragments is taken to be about ten percent of the size scale of the flow opening itself. This is consistent with observations.[37,44] It is also consistent with the approximate size scale of the turbulence in the liquid. This initial fragment size does not typically satisfy Eq. (3-3) so that further atomization will take place.

To estimate the droplet size as a function of time past initial breakup two things are needed. The first is an estimate of the time needed to breakup, for a droplet of a given size with a given relative velocity. The second is the change in relative velocity over the estimated breakup time. With these, one can compute d(t) by assuming, for example, that each droplet breaks into n_1 smaller ones of equal size, each of which breaks into n_2 even smaller ones until the condition $N_d < N_c$ is satisfied.

A relation for $u_r(t)$ may be estimated by the solution to the force-acceleration equation for a spherical droplet.

$$\left(\frac{\pi}{6} d^3\right) \rho_\ell \dot{u}_r = - \left(\pi \frac{d^2}{4}\right) \frac{c_d \rho_g}{2} u_r^2$$

where ρ_ℓ is the liquid density, c_d is the drag coefficient and the absolute velocity of the surrounding gas has been assumed constant during an individual fragmentation event, though it is certainly not constant over the whole course of the aerodynamic atomization. The non-dimensional solution is

$$\frac{u_r}{u_{ro}} = \left[\frac{3}{2}\frac{\rho_g}{\rho_\ell}\frac{u_{ro}}{d}\,t + 1\right]^{-1} \qquad (3\text{-}4)$$

where $u_{ro} = u_r(0)$ and in which a drag coefficient of 2.0 has been used. Hence the rate at which the droplet velocity equilibrates to the gas velocity varies directly with d and inversely with u_{ro}.

An estimate of the breakup time t_b can be obtained by calculating the deformation velocity v and solving

$$\frac{d}{2} = \int_o^{t_b} v\,dt \quad .$$

Here it has been assumed that the deformation taking place is the flattening of a sphere and that rupture occurs when its minor axis diameter is d/2. The velocity v is then the velocity of the sphere surface relative to its center of gravity and may be estimated at least semi-quantitatively from

$$\left(\frac{\pi}{6}d^3\right)\rho_\ell\,\dot{v} = \left(\frac{\pi}{4}d^2\right)\frac{c_d\rho_s}{2}\,u_r^2 - \left(\pi d^2\right)\frac{f\sigma}{d}$$

where

$$f = \frac{1}{4}N_c$$

must be taken to agree with the Weber number criterion.

The solution of v(t) is

$$v = (u_{ro} - u_r) - \frac{6f\sigma t}{\rho_\ell d^2}$$

which gives an estimate of t_b as

$$t_b = \left(\frac{3}{2}\frac{\sigma}{\rho_\ell d^2}\right)^{-1/2} [N_{do} - N_c]^{-1/2} , \qquad (3\text{-}5)$$

where N_{do} is the initial Weber number.

Now d(t) may be estimated by specifying values for d_i and u_{ro}. Given these, one may proceed as follows to obtain d(t). Starting with $d = d_i$ one can compute t_b from Eq. (3-5). Then with $t = t_b$ Eq. (3-4) will give the change in relative velocity over the time t_b. Now with $d = d_i(n_i)^{-1/3}$ and the new value of relative velocity given by $u_{ro} = u_r(t_b)$ the process can be reiterated for new values of t_b and $u_r(t_b)$ etc., until the condition $N_d < N_c$ is satisfied. The solution is now seen to depend on d_i, u_{ro}, and n^*. As already discussed, d_i can be taken as $d_i = 0.1D_o$ for a rough opening, where D_o is the size of the flow opening. If the vapor into which the jet is injected is quiescent and any effect of entrainment is neglected, then u_{ro} is approximated by the liquid velocity at the exit. The number of fragments resulting from a breakup event j, say n_j, depends on N_d. Experiments have shown that any liquid droplet suddenly introduced to a moving gas stream, such that $N_c < N_d \tilde{<} 20$, will begin to deform.[22] The deformation begins as a flattening of the droplet with the largest cross-section oriented normal to the gas flow. Eventually the flat shape "inverts" so as to form a bag or parachute-shaped object with the opening of the bag facing upstream. The rim of the bag is seen to contain the major part of the liquid mass since the part forming the bag is a thin film of liquid. Eventually the bag bursts and the thin film ruptures into a spray of tiny droplets and the more massive rim breaks into about five to ten droplets.[24,45] For $N_d > 20$, a much different type of disintegration process is observed. In this case a spray of tiny drops is stripped away from the surface of the drop before any deformation of the bag type can take place.[22,45] In this case the number of droplets produced from the disintegration event is typically around 50. Hinze points out that there is a gradual transition between these two types of single-droplet disintegration events as N_d varies.[22] To account for this variation in disintegration type a linear variation has been selected for the calculations reported here. It has the form

$$n_j = 5 + \left(\frac{N_d - N_c}{20 - N_c}\right) 50 \qquad (3\text{-}6)$$

and is limited to a maximum value of 50.

The only remaining item to be specified before the calculations can be performed is the critical Weber number N_c. The experimental data of Lane[27] are particularly useful for this purpose. Lane obtained the critical Weber number for water droplets under "steady" and "transient" conditions. For the steady N_c, drops of water were introduced into the steady flow of air in a wind tunnel. For the transient N_c, stationary droplets were subjected to the sudden blast of a shock wave in air. Lane's key observation was that in the steady flow case, N_c was constant and had a value of about 9; in the transient flow case N_c was shown to decrease roughly linearly with the velocity of the air behind the shock wave.[27] The latter behavior is to be expected according to the early linear analysis of Hinze.[20,21] The later nonlinear analysis of Simpkins[45] places even more weight on the experimental findings of Lane.

For the purpose of this study, a simple expression for N_c can be obtained from dimensional analysis. Suppose that the "stripping" disintegration mode is predominant under the transient conditions expected in a liquid jet. Then to be significant, the shear force at the surface of liquid fragments would be expected. The competition between the shearing force and surface tension force can be expressed by the number N_u where

$$N_u = \frac{\nu \rho_\ell u}{\sigma}$$

where ν is the kinematic viscosity of the liquid and the characteristic length scales for the velocity gradient and the droplet size are considered equal. Since aerodynamic pressure forces are still important, one would expect the product $N_c N_u$ to be roughly constant. This quantity is computed using Lane's data and listed in Table III-2. In this table u is the relative velocity under transient conditions below which disintegration does not take place. The product $N_c N_u$ has an average value of 1.1 with a standard deviation of 26% of the mean for Lane's data. Since the number $N_c N_u$ depends on the cube of the velocity, and since Lane expressed a degree of uncertainty in measuring u, this deviation can be considered well within the experimental error.

TABLE III-2

CALCULATION OF $N_c N_u$ USING THE DATA OF LANE FOR WATER DROPLETS IN AIR

d(cm)	u(cm/s)	N_c	$N_c N_u$
0.4	1200	8.23	1.41
0.3	1210	6.28	1.09
0.2	1260	4.54	0.82
0.1	1600	3.66	0.84
0.05	2400	4.10	1.41

For the purpose of testing the foregoing simple atomization model, calculations were performed for the experimental configuration of Nagaosa et al.[33] These workers injected water through a 0.071 cm diameter orifice into air at various relative flow speeds. Table III-3 compares the computed size with the measured mean drop size for four flow speeds. Since the experiments used a carefully machined orifice, d_i was chosen somewhat arbitrarily as 0.035 cm rather than 0.0071 as expected from a rough flow aperture. The remaining parameters used for these calculations are $\nu = 0.01$ cm^2/s, $N_c N_u = 1.1$, $\sigma = 71$ dynes/cm, $\rho_\ell = 1.0$ g/cm^3 and $\rho_g = 1.0 \times 10^{-3}$ g/cm^3. Computer printouts of these calculations are listed in Appendix B. Clearly the computed values for droplet scale given in Table 1II-3 are within about 20% of the measured values for mean droplet size.

The next step is to compute the expected size scale and time scale for atomization under typical, non-flashing SGTR conditions. For this purpose, the following typical conditions were selected: exit velocity $u_{ro} = 1.0 \times 10^4$ cm/s; size

TABLE III-3

COMPARISON OF COMPUTED DROPLET SCALE WITH THE MEASUREMENTS OF NAGAOSA ET AL.

u_{ro}(cm/s)	Measured Droplet Scale (cm)	Computed Droplet Scale (cm)	Atomization Time (s)
3.6×10^3	6.5×10^{-3}	8.1×10^{-3}	9.4×10^{-4}
3.9×10^3	5.6×10^{-3}	7.1×10^{-3}	4.8×10^{-4}
4.6×10^3	5.8×10^{-3}	5.7×10^{-3}	3.1×10^{-4}
4.9×10^3	4.3×10^{-3}	5.2×10^{-3}	2.8×10^{-4}

scale d_i = 0.1 and 1.0 cm, liquid kinematic viscosity $\nu = 1.0 \times 10^{-3}$ cm^2/s, exit liquid density $\rho_\ell = 0.69$ g/cm^3, ambient gas density $\rho_g = 0.055$ g/cm^3 and $N_c N_c$ = 1.1. Of the results for the two initial size scales exhibited in Table III-4, we think that the results for d_i = 0.1 cm are more typical of SGTR conditions. Note that the final equilibrium size is fairly insensitive to the magnitude of d_i.

The results of Table III-4 show, to the extent that one can believe the crude aerodynamic atomization model presented here, that a size scale close to a micron in magnitude can be produced by aerodynamic atomization in the available transient time between the rupture opening and any surrounding structure. The reason for this is that during the atomization process, N_d is much greater than N_c meaning that the droplet stripping mode of disintegration is predominant. This mode is known to produce a finer spray than the bag disintegration mode,[22] a fact that is reflected in the results. Another important reason for the small size scale at SGTR conditions is that the surface tension is only 12 dynes/cm compared to 71 dynes/cm at atmospheric pressure.

Brown and York measured a mean droplet size of 8.9×10^{-5} cm for a flashing water jet issuing from a 0.1 cm sharp-edged orifice at 414 K from a vessel at 8.2 bar (assumed to be a gauge pressure). The corresponding exit velocity for these experimental conditions was 2.38×10^3 cm/s. Assuming d_i = 0.05, the foregoing model for aerodynamic atomization gives a droplet size scale of 1.9×10^{-2} cm, about two orders of magnitude larger than the measured size. As expected then, there must be an alternative mechanism producing the much smaller droplets in a flashing jet. "Boiling breakup" is one such mechanism and is the subject of the next section.

D. Boiling Breakup

The concept of "boiling breakup" as an important atomization mechanism was introduced by Crowe and Comfort.[12] The basic idea is that a superheated droplet

TABLE III-4

COMPUTED SIZE SCALE AND ATOMIZATION TIMES FOR SGTR CONDITIONS

d_i (cm)	Size Scale (cm)	Time Scale (s)
0.1	1.5×10^{-4}	4.5×10^{-5}
1.0	4.0×10^{-4}	4.5×10^{-4}

will eventually begin boiling at points internal to the droplet. (Note that homogeneous nucleation is necessary for this to happen.) Any vapor formed internally will then have the tendency to disrupt and rupture the droplet. The smaller droplets formed from this rupture process will also be subjected to internal boiling, provided they are still superheated. Thus a cascading rupture process proceeds until a pressure jump condition due to surface tension at the droplet surface is satisfied. This jump condition is expressed by Crowe and Comfort as

$$\left(\frac{4\sigma}{d} + p_o\right) > p_s(T) \tag{3-7}$$

where p_o is the pressure external to the droplet and $p_s(T)$ is the saturation pressure at the droplet temperature T.

Just as for aerodynamic breakup, the dynamics of the boiling breakup process can be examined with the aid of calculations for a set of idealized circumstances. Consider for this purpose a spherical liquid droplet with mean temperature T_o greater than the external saturation temperature $T_e(p_e)$ of its vapor at pressure p_e. This droplet, having been formed in the initial breakup process, must have a surface temperature of essentially T_e. Since $T_o > T_e$ there will be a radial temperature distribution in the droplet established through thermal diffusion which varies with time, but nonetheless always has its maximum at the droplet center. Because the probability of homogeneous nucleation occurring increases with temperature, the most likely thing to happen is that a single vapor bubble will begin to grow at the droplet center. The vapor formed at the droplet center will be at a pressure p corresponding to a temperature greater than T_e so that $p > p_e$, causing the bubble and therefore the droplet to expand. Assuming the bubble growth limiting process to be the inertia of the spherical liquid annulus surrounding the vapor bubble at the droplet center, the following system of dynamical equations may be written:

$$\frac{dr}{dt} = u$$

$$m_\ell \frac{du}{dt} = (p - p_e)A - \left(\frac{2\sigma}{r}\right) A$$

$$m_\ell c \frac{dT}{dt} = -\frac{kA}{r}(T - T_e) - L\frac{dm}{dt}$$

$$\frac{dm}{dt} = \frac{d}{dt}(\rho_s V_s)$$

$$V_s = \frac{4}{3}\pi(r^3 - r_o^3)$$

$$m_\ell + m = m_o \quad . \qquad [3\text{-}8(a\text{-}f)]$$

Here r(t) is the outer radius of the expanding droplet, u(t) is the velocity with which it expands, $m_\ell(t)$ is the remaining liquid mass, m(t) is the mass of vapor formed in the bubble, $V_s(t)$ is the volume of the internal bubble, $A(t) = 4\pi(r/2)^2$, $\rho_s(t)$ is the vapor density in the bubble, r_o is the constant starting radius, and m is the constant mass of the droplet-bubble system. The small fractional variation in m_ℓ has been ignored on the left hand side of Eqs. (3-8b) and (3-8c) and in Eq. (3-8e) in the derivation of the preceeding equations. Also the constants k, c, L, and c_{ps} are the thermal conductivity of water, heat capacity of water, latent heat of evaporation of water, and constant pressure specific heat of the steam. Equations [3-8(a and b)] express the radial motion of the liquid, Eq. (3-8c) is an energy equation for the liquid and Eqs. [3-8(d-f)] are supplementary. Closure can be obtained by using the best-fit expressions for Steam Table data[40]

$$p = \left(\frac{T - 255.2}{117.8}\right)^{\frac{1}{0.223}} \times 10^6$$

$$c_{ps} = 9.5875 \times 10^6 \left(1.0 - \frac{T}{647.3}\right)^{-0.8566}$$

$$\rho_s = \frac{p}{0.3 c_{ps} T} \quad . \qquad [3\text{-}9(a\text{-}c)]$$

By specifying values for the constants, in addition to an initial value for the liquid temperature, the system given by Eqs. (3-8) and (3-9) can be integrated numerically. The numerical procedure is described in Appendix C.

To obtain results with this, an assumption as to the volume at which the droplet will rupture must be made. For the purposes of this scoping analysis, rupture is assumed to occur when the droplet-bubble system has doubled its origi-

nal volume. Then the bubble radius will equal the starting radius of the droplet. Furthermore, a cascading rupture calculation (similar to that which was performed in the previous section on aerodynamic atomization) can be made by computing the likely number of droplets to arise from the rupture n. The time to reach an equilibrium size will then be simply the total time needed to rupture a set of increasingly small droplets by internal bubble growth.

The number of droplets to result from a disintegration event n_j can be estimated by realizing that the interface between the internal bubble and the droplet will be Rayleigh-Taylor unstable. Ishii[24] gives the predominant wave length of this instability λ_m as

$$\lambda_m = 2\pi \sqrt{\frac{3\sigma}{a(\rho_\ell - \rho_v)}}$$

where a is the magnitude of the acceleration of the interface. If the initial droplet size is d_j, then the size of the internal bubble at rupture will be d_j. The number of resulting droplets can be estimated by the number of predominant wave lengths that will fit into d_j. For this we select an area-ratio basis. Hence,

$$n_j \sim \frac{\pi d_j^2}{\lambda_m^2} = \frac{d_j^2}{4\pi}\left(\frac{3\sigma}{a(\rho_\ell - \rho_g)}\right)^{-1} \qquad (3\text{-}10)$$

where a can be taken as the average of r(t) during the expansion process. The droplet size resulting from disintegration event j is then

$$d_{j+1} = d_j n_j^{-1/3}$$

and so on.

The results of calculations using the cascading boiling breakup model just described are given in Table III-5 together with the results of aerodynamic breakup calculations. Computer printouts for these calculations are listed in Appendix C. Four sets of conditions were computed, one each for the experimental conditions of Brown and York[5] and those of Alger and Geidt,[2] as well as results

TABLE III-5

COMPARISON OF ATOMIZATION CALCULATIONS

Conditions	d_i(cm)	Aerodynamic d_e(cm)	Aerodynamic t_e(s)	Boiling Breakup d_e(cm)	Boiling Breakup t_e(s)	Measured Size (cm)
Brown & York		(a)		2×10^{-4}	7×10^{-6}	9×10^{-5}
T_o = 414 K	0.01	2×10^{-2}	7×10^{-4}			
ΔT_s = 41 K	0.10			3×10^{-4}	2×10^{-5}	
Alger & Geidt						
T_o = 443 K	0.06	(b)		1×10^{-4}	1×10^{-5}	2×10^{-4}
ΔT_s = 66 K	0.10	(b)		1×10^{-4}	2×10^{-4}	
SGTR						
T_o = 590 K	0.1	2×10^{-4}	5×10^{-5}	4×10^{-4}	9×10^{-6}	-
ΔT_s = 31 K	1.0	4×10^{-4}	5×10^{-4}	8×10^{-4}	9×10^{-5}	
T_o = 580 K	0.1	2×10^{-4}	5×10^{-5}	1×10^{-3}	1×10^{-5}	
ΔT_s = 21 K	1.0	4×10^{-4}	5×10^{-5}	4×10^{-2}	1×10^{-4}	
T_o = 562 K	0.1	2×10^{-4}	5×10^{-5}	(a)		-
ΔT_s = 2 K	1.0	4×10^{-4}	5×10^{-5}	(a)		

(a) Droplets initially smaller than the equilibrium size.
(b) An initial relative velocity could not be determined from the description of the experiment.

for three sets of SGTR conditions. Because of the order-of-magnitude analysis employed, the results are reported using only one significant figure. It is clear that agreement is good within a factor of about three with measurements in widely disparate experimental circumstances. The droplet size data of Brown and York were obtained for a flashing jet issuing from an orifice. The size data of Alger and Geidt were taken in the steam-water mixture emerging from a converging-diverging channel, into which flowed a very low quality ($\theta \sim 0.987$) saturated steam-water mixture.

The key feature of the calculations shown in Table III-5 is that for each of the SGTR conditions computed, the smallest equilibrium droplet size d_e is obtained with the aerodynamic (non-flashing) atomization mode. In fact, for the case of $\Delta T_s = 2$ K, the d_e due to aerodynamic forces is two to three orders of magnitude smaller than that due to boiling breakup. This result can be understood on the basis of the physical mechanisms being modeled. First, it is clear from Table III-5 that d_e decreases with increasing superheat as expected. However there also seems to be a tendency toward larger d_e at the higher pressure of SGTR conditions. This tendency was confirmed by a series of calculations for $p_e = 1$ bar and $p_e = 70$ bar at varying ΔT_s. The result is given in Fig. 3-2. For both external pressures d_e varies inversely with ΔT_s, but d_e is generally greater for the higher external saturation pressure condition. The reason for this is that the lower surface tension at the high pressure (and therefore temperature) causes droplets to disintegrate into many more fragments than at equivalent ΔT_s at lower external saturation pressures. The early creation of small droplets means that the droplets can lose their superheat through heat conduction at a more rapid rate. This effect terminates the boiling breakup process earlier than would be the case at lower external pressures.

The main point of significance here is that whereas boiling breakup can be an important atomizing mechanism at low external pressures, it may not be the dominant mechanism at SGTR pressures. However an alternative perspective on boiling breakup can be envisioned which may reverse this finding. In the boiling breakup model just described, an initial disintegration of the metastable liquid water column has been assumed to occur due to roughness of the rupture opening. One can imagine that if the metastable liquid were to undergo a more-or-less uniform homogeneous nucleation, even prior to an initial breakup, the equilibrium droplet size could be attained in a single step. This could be so if the number of nucleation sites were large, since the scale of droplet size resulting from

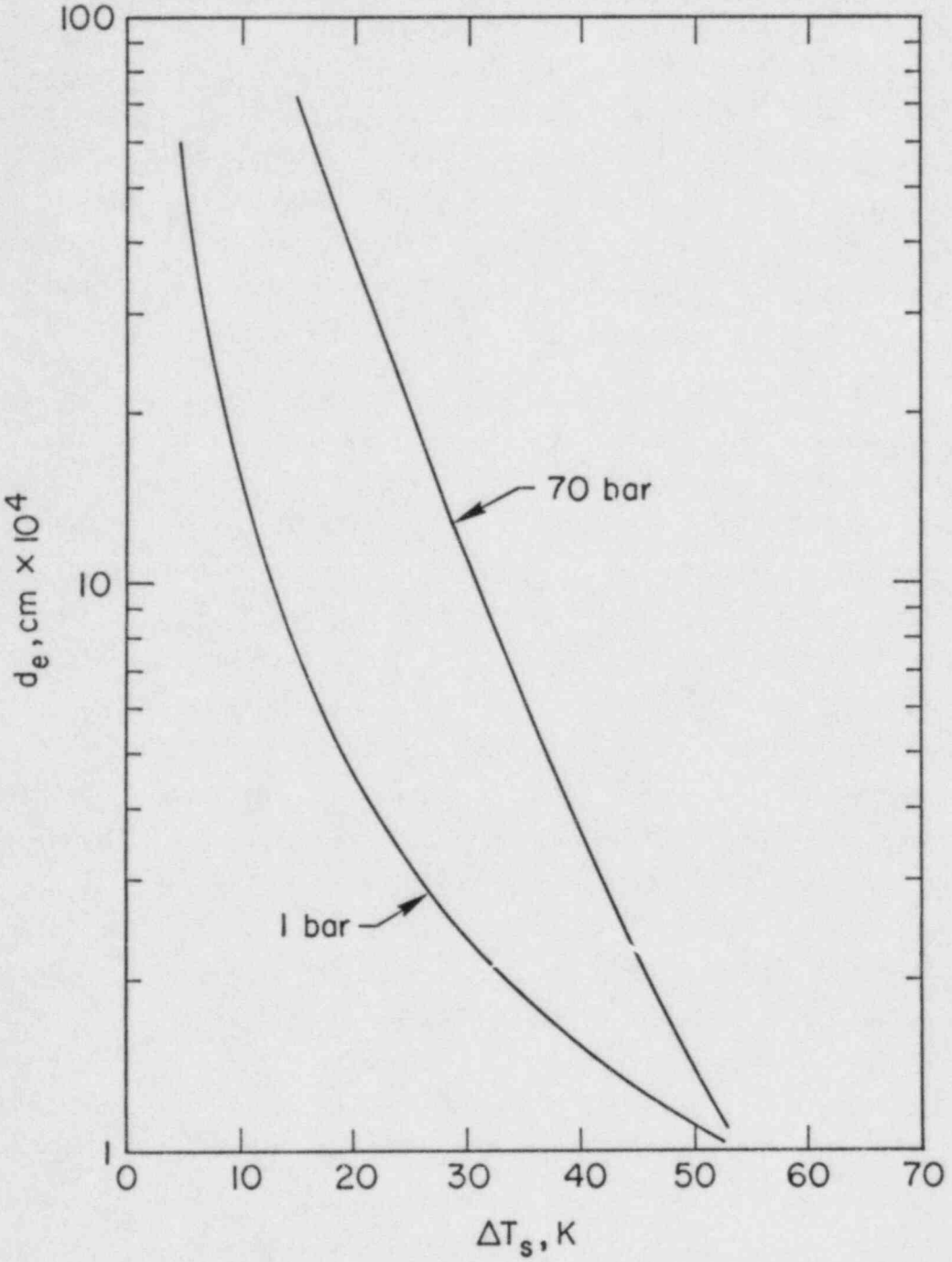

Fig. 3-2. d_e vs ΔT_s for boiling breakup model under SGTR conditions.

the close-packing of many bubbles is given roughly by $N^{-1/3}$ where N is the number density of nucleation sites. For homogeneous nucleation, values of N of 10^{12} cm^{-3} are not uncommon[40,42,46,50] so that an initial scale of 10^{-4} cm resulting from the explosive disintegration of the meta-state liquid could be realized.

Hence boiling breakup may or may not play a diminutive role in atomization at SGTR conditions; nonetheless if the primary fluid exits with the expected velocity ($\sim 10^4$ cm/s), then aerodynamic disintegration could very well produce droplets of about one micron in size. As seen in the previous section the aerodynamic disintegration criteria N_c depends on the square of the relative velocity. Hence an actual exit velocity somewhat smaller than 10^4 cm/s could produce a much larger droplet size scale. For this reason the potential of further fragmentation due to collisional processes should be addressed. This is the subject of the next section.

E. Collisional Fragmentation

There are two main ways in which collisional fragmentation can occur. The first is as a result of the encounter of one droplet with another, and the second is by the encounter of a droplet with a rigid surface such as a steam generator tube. In either case the encounter may be a direct collision or a near collision. In the event of a near collision, a force is nonetheless exerted on a droplet from the obstacle (other droplet or rigid surface) through the intervening fluid as the droplet trajectory is deflected.

For both cases of collisional fragmentation, a lower limit on the droplet size resulting from direct collisions can easily be obtained as follows. Consider the case in which all of the kinetic energy of the motion of a droplet of size d_i relative to the obstacle is converted to potential energy of surface tension. If the encounter is a direct droplet-droplet collision, then this corresponds to two droplets colliding with relative velocity u_r and fragmenting into many little droplets with zero velocity relative to one another. If the encounter is with a solid surface, the case under consideration corresponds to a droplet impacting the surface, coming to a complete rest on the surface and breaking, with all subsequent little droplets remaining at rest. The result of the energy balance in this case is found to be independent of d_i, and can be expressed as

$$\frac{\rho_\ell u_r^2 d}{\sigma} = 12$$

where d is the fragmented droplet size.

To estimate d arising from a droplet-droplet collision the relevant u_r must be estimated. Tsuji and Morikawa[52] have measured the magnitude of the turbulent fluctuations in velocity for solid particles in turbulent air. They find that the fluctuating part of the velocity is roughly 10% of the mean particle velocity. Since collisions can be expected to occur as a result of turbulent fluctuations, as well as a result of droplets streaming past one another due to a spectrum in droplet sizes (and therefore a spectrum in droplet velocities), this will serve as at least one estimate. The result for SGTR conditions, assuming a mean droplet speed equal to the speed of the liquid column of the jet, is a droplet size of 2×10^{-4} cm. (At SGTR conditions, $\rho_\ell \sim 0.7$ g/cm^3 and $\sigma \sim 12.5$ dynes/cm.)

If on the other hand droplet streaming produces the important relative velocity, another estimate can be made. The velocity of the droplets will in general depend on their size, so that the mean relative velocity will depend on the breadth of the size distribution function. The nature of the size distribution function will depend heavily on the dominant atomization mechanism. For example, if uniform nucleation at 10^{12} sites per cubic centimeter occurs, a relatively sharp distribution in size may be expected. However, if aerodynamic atomization were to dominate, then a rather broad distribution could be expected. Without delving into the matter further, one could suppose the relative velocity for a collection of droplets with a wide size range to be somewhat greater than the relative velocity due to purely turbulent fluctuations. The tendency would be to produce collision fragments somewhat smaller than 2×10^{-4} cm.

In the case of droplet-tube collisions, the droplets that manage to impact a neighboring tube or other structure will do so with whatever is their current absolute velocity. From the aerodynamic atomization calculations, this was seen to be typically about 2×10^3 cm/s at times comparable to the rupture-to-tube transit time. This gives a size scale of 5×10^{-5} cm.

These estimates all produce sizes comparable to, or smaller than anything to be expected from either the aerodynamic or boiling breakup mechanisms discussed previously. The estimates are also very conservative in that they represent a lower bound on that which can be expected in reality. This is due to the assumptions of direct collisions, total conversion of kinetic energy to surface

energy, and the nature of the relative velocity estimates. The estimates show, however, that the important collisional fragmentation processes for further study are encounters between drops of differing size (and therefore differing velocity) and encounters of drops with solid structure.

What remains to be done now is to refine the estimates of d resulting from collisional fragmentation. The actual splashing process is characterized by a very complex redistribution of the incoming kinetic energy of a droplet.[45,53] This kinetic energy is shared among the energy of surface tension of a set of smaller fragments together with their total kinetic energy leaving the encounter and any added dissipative heat produced from deformation during actual breakup. A thorough study of the sort needed to obtain a secure picture of the splashing process would be very extensive. This is especially so when the splashing may be for a liquid on a very hot surface, as in the near rupture region in SGTR accidents. Also, there is a significant indication that drops on the 10^{-4} cm size scale may result purely from atomization. Therefore the results of the bounding calculations for collisional fragmentation performed in this section will be left to stand as the conclusions of this part of the investigations until the necessity for additional detail is indicated by subsequent parts of the overall study.

F. Drop Size Distributions

This section serves to indicate the factors determining the nature of the droplet size distribution function within the context of the foregoing analysis.

It has been shown that the droplet size produced by cascading boiling breakup depends mainly on the initial temperature difference of the discharged liquid above that of the ambient. The mean temperature of the discharge and its spatial or volume distribution will depend on the rupture location. In general there will be two streams of primary fluid arriving at the rupture site, one from the hot-side plenum and another from the cold-side plenum. These plenums are at different temperatures, pressures and flow distances from the rupture site, and therefore they will supply discharge fluid just before the exit at two different velocities and temperatures. Because the exit region is very short, little mixing of these two streams can be accomplished prior to their leaving the pipe and forming the flashing jet. Hence the temperature distribution will be essentially bimodal with the amount of fluid in each mode determined by the velocities of the two streams arriving at the tube exit. A method for determining these two flow speeds, based on the Darcy-Weisbach equation and an assumed exit impedance, is given in Appendix D. With these velocities, the temperatures of the joining streams can be computed using the results of Sec. II.

The bimodal distribution in droplet size, formed by boiling breakup of the liquid column with a bimodal temperature distribution, will then be subject to attaining a distribution in droplet velocities. This is because the velocity of the smaller droplets will tend to the surrounding gas velocity more strongly than will the velocity of the larger ones. This velocity distribution will in turn be altered as the droplets are subjected to collisional fragmentation.

If the dominant atomization mechanism is aerodynamic disintegration, as expected from the results of Sec. III-C, then the distribution in droplet size may be determined from existing experimental correlations. For this purpose, results of studies such as that of Mugele and Evans[32] can be employed.[16,31]

With these results the study must now turn to questions of how the flashing liquid jet disintegrates under submerged conditions. This is the subject of the next section.

G. Flashing Jet Under Submerged Conditions

The computerized literature survey conducted for this study, on the subject of flashing submerged jets, indicated no reference to activity since 1970 for the data bases searched. Subsequent word-of-mouth probing around the current multiphase flow community showed that apparently no definitive experimental or theoretical work has been done in the case of sustained flashing of a superheated liquid jet injected into a subcooled liquid.

The only potentially relevant material to emerge from these searches of the literature concerns the injection of a gas into a liquid, a practice followed frequently in metal refining. In this connection Oryall and Brimacombe[36] and Themelis et al.[51] each conducted flow studies in which air was injected into water for the purpose of studying the physical behavior of the jet. The general behavior is as follows.

Immediately upon leaving the injection point, a frothy mixture of small bubbles (about the size scale of the flow opening) and water forms a diverging jet. If the injection is horizontal, the jet remains generally horizontal as it diverges with an angle of about 20 degrees. Gradually the directed motion of the jet is slowed to the point where buoyancy forces dominate and the jet turns as a whole until it rises vertically as a two-phase plume. The 20 degree divergence angle is approximately constant with increasing injection speed due to the increasing effect of turbulent mixing with increasing velocity, just as in a single-phase jet.[30,36,51]

The question here is whether or not a flashing superheated liquid jet will give rise to a similar sort of behavior when injected into its own subcooled liquid, as may be the case for primary fluid discharge for the greatest share of a SGTR accident. The tentative answer is that the flashing jet will behave in a generally similar manner forming a frothy mixture of small steam bubbles in water. The primary rationale behind this conclusion lies in the idea that the submerged flashing jet will likely exhibit an intermittency. The natural intermittency of a flashing jet will probably be aggravated by vibrations and pipe whip in the ruptured tube resulting from interaction of the two-phase jet with surrounding tubes and steam generator structure. This intermittency of the injection means that surrounding liquid will be alternately pushed away from and flooding into the immediate region of the tube rupture. The attendant instability of the low-density steam accelerating the high-density water gives plenty of opportunity for bubble formation. The frequency of oscillations in this system is expected to be high because of the relatively rigid support of steam generator tubes. This high frequency should be accompanied by a correspondingly small scale in bubble size.

The relevance of the foregoing thinking is that the existence of the froth, rather than a large vapor space surrounding the rupture site,[9,39] may preclude any formation of tiny primary fluid droplets. Alternatively, if droplet formation is somehow achieved, any droplets in the small bubbles may impact the walls of the bubble and mix with the secondary side water with such completeness that essentially no primary fluid will reside in tiny droplets. The reason for this is that a bubble is slowed by the surrounding water much more rapidly than a droplet inside a bubble can conform to changes in the bubble speed.

In SGTR accidents in which the steam generator fills with water, the likelihood of the rupture site becoming submerged very early in the transient is high. For such cases it may become exceedingly difficult for primary fluid to escape the steam generator in the form of tiny droplets during times of ARV opening.

It should be heavily emphasized that this possibility is only suggested by a set of qualitative arguments based on the idea that a submerged flashing jet will have a behavior similar to a gas jet injected into a liquid. The potential importance of this mechanism in insuring against radioactivity release in SGTR accidents suggests that a fundamental set of experiments should be conducted to qualify or dispute the foregoing ideas.

IV. FLOW THROUGH THE TUBE BUNDLE TO THE SEPARATOR REGION

In the previous sections, the potentiality of producing droplets of primary fluid on the scale of 10^{-4} cm in the damaged steam generator has been examined. The findings of these studies are most conclusive in the case of SGTR accidents in which the tube rupture location and the state of the steam generator environment are such that primary discharge takes place into a vapor-filled space. In such cases, the bulk of the discharged primary fluid is expected to be in droplets on the size scale of 10^{-4} cm. In the more likely event that accident conditions are such that the primary discharge enters a liquid-filled steam generator space the findings are inconclusive. Further judgement on this facet of SGTR accidents must await results from the important experiments currently under way at Northwestern University and conducted by Bankoff.[3] Prior to the availability of these new data, it is nonetheless possible and appropriate to speculate on what may be found.

The Bankoff experiments are designed to simulate the main hydrodynamic feature of SGTR transport phenomena. The scheme is to flow a well-defined steam-water mixture through a vertical conduit containing a set of axially oriented rods. This is to represent a small segment of the steam-generator tube bundle. The quality and flow speed of the upward-moving steam-water mixture can be varied so as to simulate a wide variety of steam generator conditions, both before and after reactor scram.

The simulated injection of primary fluid takes place through an orifice located in the side of the conduit and fed by a tube connected to a high-pressure vessel containing the hot primary fluid. The pressures are in general much lower than prototypical pressures, but are scaled in such a way as to maintain mass flux similarity. A tracer system is employed that enables a mass balance to be performed, after having collected the mixture leaving the conduit and measuring that which remains in the conduit after allowing the system to flow for a period of time. This provides a measure of how much the net upward flux of primary fluid in liquid form is diminished in a unit length of the steam-generator tube bundle.

Of key importance in these experiments is the ability to inject the primary fluid into either pure vapor or pure liquid spaces of the conduit.

On the basis of the analysis and discussion of the previous sections, the following speculations can be made concerning distribution of primary fluid in these future experiments. For discharge into a vapor space one can expect essen-

tially all of the primary fluid to escape the conduit. This is because 10^{-4} cm droplets can be expected to follow the streamlines of the steam flow with essentially perfect fidelity. It should be noted however, that for production of prototypical-sized droplets the quantity

$$\frac{\rho_g u^2 D}{\sigma}$$

must be prototypical. Here u is the primary exit speed through an orifice of size D. If a steam generator pressure significantly lower than 70 bar is used, then the surface tension of the simulated primary fluid may have to be artificially altered so as to maintain this similarity.

For discharge into a pure liquid space, the far-reaching speculation is that little or no primary fluid will escape the conduit. In this case total "washing out" of any primary fluid droplets may occur. The only potential for droplet formation will be at the surface of the pool where droplet formation due to bursting bubbles during pool boiling may occur. Since the velocity of vapor leaving a boiling pool surface is much smaller than that at the discharge orifice, considerably larger droplets are likely to form in this case. In addition the concentration of primary fluid in any such droplets will be diluted due to prior mixing with secondary fluid. The large size[1] and low concentration of primary fluid in these drops both work toward decreasing the amount of primary liquid capable of escaping the simulated steam generator section. If the liquid level is very far below the top of the conduit where the steam exits, then it is possible that essentially no liquid mass can leave the conduit. Again it is important to realize, however, that surface tension is an important property in determination of droplet size in pool-boiling too. Hence similarity of important non-dimensional quantities is essential in these experiments.

V. RELEVANCE TO OTHER SGTR STUDIES AND RECOMMENDATIONS

A number of points have emerged in the course of this study that are connected in some way to other SGTR research programs. In some cases the results of the foregoing analysis will influence other studies and vice versa. This section is a catalog of these related areas.

First, regarding best-estimate system calculations, it was seen in Sec. III-B that a small difference in temperature of the primary fluid could mean the

difference between flashing and non-flashing at the rupture site. Since the uncertain formation of a large vapor space under submerged discharge conditions depends on flashing at the rupture site, an accurate knowledge of this temperature is needed.

On the question of flow rate limiting mechanism, it should be emphasized that whether or not critical flow occurs is highly dependent on the rupture geometry. It has been shown that if the rupture occurs as an axial tube slit whose area is smaller than the tube cross section, critical flow is unlikely. If, however, the rupture configuration is such that an internal flow distance of at least one or two tube diameters is available downstream of the point where saturation pressure is first reached, critical flow of some sort can be expected. This could be the case, for example, if the steam generator tube were to shear off at the tube sheet. Therefore in computation of SGTR accident effects, one must be careful to consider exit location and geometry effects.

In the previous section the matter of maintaining Weber number similarity was discussed. The importance of this matter should not be overlooked, particularly in experimental programs.

The idea of acceleration-influenced homogeneous nucleation is, as far as can be determined, a new concept in nucleation theory. Its importance to SGTR accidents relates to understanding the mechanism of droplet formation in a flashing jet. Added confidence in the theory could be obtained by a more in-depth theoretical study. Such a study could also seek to predict the likely number density of active nucleation sites under accelerating circumstances.

The question of the breadth of the droplet size distribution was only touched upon in this study. At present the efficiency of the steam dryers and separators of current steam generators is fairly well-defined for normal operating conditions. However under the transient conditions the droplet removal efficiency of these devices is less well known. For this reason experimental programs such as the MB-2 Transient Test Program have been planned.[54] It remains to be seen from these tests whether added detail is needed in describing the drop size distribution. However, it is important to point out that a simulated rupture geometry should be selected that maintains prototypical droplet formation mechanisms. To achieve this, a prototypical rupture geometry is needed. By the term prototypical rupture geometry we mean that the final area reduction should occur at the end of any simulated ruptured tube. In this way the metering of the rupture flow will be a result of the rupture itself and atomization can take place as it would under actual SGTR circumstances.

Throughout this study the assumption has been made that the radioactive materials dissolved in the primary fluid are essentially non-volatile. Therefore the main potential for radioactivity release has been assumed to be through release of primary fluid. To test the validity of this assumption, Oak Ridge National Laboratory (ORNL) has been charged with determining the equilibrium partition coefficient for radioiodine in a steam-water system at realistic conditions of pressure, concentration, and acidity.* The importance of a careful determination of the volatility property should not be underemphasized. The ORNL results should be carefully examined and folded into future thermal-hydraulic SGTR studies.

Finally the matter of determining the physical behavior of a submerged flashing jet may emerge as an important and as yet unstudied physical phenomena. If the results of the Bankoff[3] experiments prove the speculations of Sec. IV to be correct, a set of detailed studies of a superheated flashing jet in its own subcooled liquid will be warranted. This is because the phenomenon may serve as an important safeguard against production of tiny droplets.

VI. CONCLUSIONS

A study has been completed in which the thermal-hydraulic facets of SGTR accidents have been probed. The main thrust has been to trace the path of primary fluid as it may pass through a ruptured steam generator tube to the steam generator and on to the atmosphere as a collection of tiny droplets in steam.

The first conclusion of the study is that, for many likely tube rupture geometries and locations, the mechanism controlling the discharge rate is probably flow impedance due to pipe friction and point losses. This is found to be likely throughout the accident transient provided the rupture occurs, as for example in the R. E. Ginna[35] accident, as an abrupt opening in the pipe with an area smaller than the pipe cross sectional area.

The second conclusion is that, given an exit velocity corresponding to roughly an 80 bar pressure differential, droplets on a size scale of 10^{-4} cm are likely to be produced at the exit. This is provided that the rupture occurs in a steam generator region that is dominated by vapor. Where the rupture occurs in submerged regions, the potential of droplet formation is unknown. However, one

*Information provided by S. D. Clinton, Oak Ridge National Laboratory, July 1984.

can speculate that this potential is small, based upon the assumption that the submerged two-phase jet is similar in behavior to a gas jet injected into a liquid.

The implications of these results for radioactivity release are the following. For combined-event accidents such as SGTR/SOSV in which the steam generator boils dry, a large share of the leaked primary fluid may reach the atmosphere in the form of tiny droplets. In more likely, single-event accidents, the total discharge of primary fluid may be contained in the steam generator. This is provided, of course, that operator response is such that the leakage is terminated prior to filling of the damaged steam generator, a situation that did not take place in the R. E. Ginna[35] accident.

ACKNOWLEDGMENTS

We wish to give our sincere thanks to Frank Harlow for having participated in forming the direction of this study and for his many helpful discussions during the course of the study. We also thank Bahram Nassersharif and Jim Lime for helping us understand the SGTR accident sequence in PWR's. Our thanks also go to Professor George Bankoff for his suggestion concerning the one-step jet disintegration mechanism.

APPENDIX A

CALCULATION OF AN EQUIVALENT POINT LOSS FOR AN ORIFICE IN A PIPE

Consider the flow section of Fig. A-1. Let A_1 be the flow area corresponding to diameter d_1, A_2 the area for orifice size d_2, u_1 the steady flow velocity in the pipe and u_2 the steady velocity at the orifice. The orifice coefficient C_o is defined by

$$u_2 A_2 = C_o A_2 \sqrt{\frac{2\Delta p}{\rho_\ell [1 - (d_2/d_1)^4]}}$$

where Δp is the pressure drop across the orifice and ρ_ℓ is the density of the incompressible fluid. If the ratio d_2/d_1 is less than about 0.1 then $(d_2/d_1)^4 \ll 1$. Using this approximation and the continuity expression

$$u_1 A_1 = u_2 A_2$$

one can write

$$u_1 = C_o \frac{A_2}{A_1} \sqrt{\frac{2\Delta p}{\rho_\ell}} \quad .$$

Rearranging for Δp gives

$$\Delta p = \left(\frac{1}{C_o} \frac{A_1}{A_2}\right)^2 \frac{1}{2} \rho_\ell u_1^2$$

from which one can identify the orifice point loss coefficient K_o as

$$K_o = \left(\frac{1}{C_o} \frac{A_1}{A_2}\right)^2 = \frac{1}{C_o^2} \left(\frac{d_1}{d_2}\right)^4 \quad .$$

Orifice in a pipe

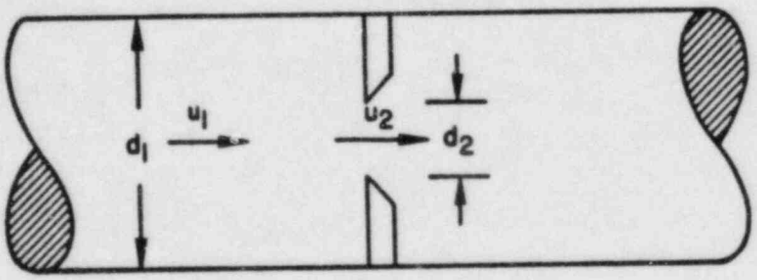

Fig. A-1

APPENDIX B

AERODYNAMIC ATOMIZATION SOLUTION ALGORITHM

The following is a FORTRAN computer program for solving the system of equations given in Sec. III-C for aerodynamic atomization of liquids.

```
      PROGRAM DARED(DOUT,TTY,TAPE1=DOUT,TAPE2=TTY)
      REAL NC,ND,KNU,NCNU
      READ(2,*) RHOL,RHOG,DI,U
      WRITE(2,40) RHOL,RHOG,DI,U
   40 FORMAT(*    RHOL=*,1PE12.2,*   RHOG=*,1PE12.2,
     1   *   DI=*,1PE12.2,*   U=*,1PE12.2)
      READ(2,*) KNU,NCNU
      WRITE(2,50) KNU,NCNU
   50 FORMAT(*   KNU=*,1PE12.2,*   NCNU=*,1PE12.2)
      SIGMA=70.9*(RHOL-RHOG)**4.
      WRITE(1,100)
      WRITE(1,110) DI,U,RHOG,RHOL,SIGMA,KNU,NCNU
  100 FORMAT(//39X,*- - - AERODYNAMIC ATOMIZATION CALCULATION - - -*//)
  110 FORMAT(*   INITIAL SIZE=*1PE9.2,*   INITIAL RELATIVE VELOCITY=*,
     1  1PE9.2,*   GAS DENSITY=*,1PE9.2,*   LIQUID DENSITY=*,1PE9.2//
     2  *   SURFACE TENSION=*,1PE9.2,*   KINEMATIC VISCOSITY=*,1PE9.2,
     3  *   NCNU=*,1PE9.2//)
      WRITE(1,115)
  115 FORMAT(3X,*STEP*,3X,*TIME*,9X,*TB*,10X,*D1*,10X,*UR*,10X,*ND*,
     1    10X,*NC*,5X,*NDROPS*,4X,*D2*/)
      C1=3./2.*RHOG/RHOL
      UR=U
      TIME=0.
      D=DI
      NC=NCNU*SIGMA/(KNU*RHOL*UR)
      NC=AMIN1(8.,NC)
      ND=RHOG*UR*UR*D/SIGMA
      IF(ND.LT.NC) GOTO 30
      WRITE(2,20) TIME,D,UR,NDROPS
      WRITE(2,45) ND,NC,SIGMA
      D1=DI
      NDROPS=0
      ITER=1
   10 CONTINUE
      C2=3./2.*NC*SIGMA/RHOL
      TB=1./SQRT(C1*UR*UR/D/D-C2/(D**3.))
      UR=UR*1./(C1*UR*TB/D+1)
      NDROPS=5+((ND-NC)/(20.-NC))*50
      NDROPS=MINO(50,NDROPS)
      D=D/NDROPS**(1./3.)
      TIME=TIME+TB
      WRITE(1,120) ITER,TIME,TB,D1,UR,ND,NC,NDROPS,D
      ND=RHOG*UR*UR*D/SIGMA
      WRITE(2,20) TIME,D,UR,NDROPS
      NC=NCNU*SIGMA/(KNU*RHOL*UR)
      NC=AMIN1(8.,NC)
      WPITE(2,45) ND,NC,SIGMA
      D1=D
      NDROPS=0
  120 FORMAT(I5,1P6E12.2,I5,1PE12.2)
   45 FORMAT(*   ND=*,1PE12.2,*   NC=*,1PE12.2,*   SIGMA=*,1PE12.2)
      IF(ND.LT.NC) GOTO 30
      ITER=ITER+1
      GOTO 10
   20 FORMAT(*   TIME=*,1PE12.4,*   D=*,1PE12.4,*   UR=*,1PE12.4,
     1   *   NDROPS=*,I5)
   30 WRITE(1,140) D1,UR,ND,NC
  140 FORMAT(*    - - EQUILIBRIUM - - *,5X,1P4E12.2//)
      STOP
      END
```

Table B-1 lists four calculations performed for the experimental conditions of Nagaosa et al.[33] Table B-2 is the calculation for the Brown and York[5] conditions, and Table B-3 gives the results for the two SGTR cases. In these tables, the units are cgs, NCNU is the product $N_c N_u$, TB is the breakup time for each step of the cascade process, TIME is the cumulated time, D1 and D2 are the beginning and ending droplet size scales for each step, and ND, NC, and NDROPS are the N_d, N_c, and number of fragments for each step respectively.

TABLE B-1

NAGAOSA ET AL.[33] CASES 1-4

INITIAL SIZE= 3.50E-02 INITIAL RELATIVE VELOCITY= 3.60E+03 GAS DENSITY= 1.00E-03 LIQUID DENSITY= 1.00E+00

SURFACE TENSION= 7.06E+01 KINEMATIC VISCOSITY= 1.00E-02 NCNU= 1.10E+00

STEP	TIME	TB	D1	UR	ND	NC	NDROPS	D2
1	3.08E-04	3.08E-04	3.50E-02	3.44E+03	6.42E+00	2.16E+00	16	1.39E-02
2	9.43E-04	6.35E-04	1.39E-02	2.78E+03	2.32E+00	2.26E+00	5	8.12E-03
- -	EQUILIBRIUM - -		8.12E-03	2.78E+03	8.90E-01	2.79E+00		

INITIAL SIZE= 3.50E-02 INITIAL RELATIVE VELOCITY= 3.90E+03 GAS DENSITY= 1.00E-03 LIQUID DENSITY= 1.00E+00

SURFACE TENSION= 7.06E+01 KINEMATIC VISCOSITY= 1.00E-02 NCNU= 1.10E+00

STEP	TIME	TB	D1	UR	ND	NC	NDROPS	D2
1	2.70E-04	2.70E-04	3.50E-02	3.73E+03	7.54E+00	1.39E+00	20	1.29E-02
2	4.80E-04	2.10E-04	1.29E-02	3.42E+03	2.54E+00	2.08E+00	6	7.10E-03
- -	EQUILIBRIUM - -		7.10E-03	3.42E+03	1.18E+00	2.27E+00		

INITIAL SIZE= 3.50E-02 INITIAL RELATIVE VELOCITY= 4.60E+03 GAS DENSITY= 1.00E-03 LIQUID DENSITY= 1.00E+00

SURFACE TENSION= 7.06E+01 KINEMATIC VISCOSITY= 1.00E-02 NCNU= 1.10E+00

STEP	TIME	TB	D1	UR	ND	NC	NDROPS	D2
1	2.14E-04	2.14E-04	3.50E-02	4.41E+03	1.05E+01	1.69E+00	29	1.14E-02
2	3.15E-04	1.00E-04	1.14E-02	4.17E+03	3.14E+00	1.76E+00	8	5.70E-03
- -	EQUILIBRIUM - -		5.70E-03	4.17E+03	1.40E+00	1.86E+00		

INITIAL SIZE= 3.50E-02 INITIAL RELATIVE VELOCITY= 4.90E+03 GAS DENSITY= 1.00E-03 LIQUID DENSITY= 1.00E+00

SURFACE TENSION= 7.06E+01 KINEMATIC VISCOSITY= 1.00E-02 NCNU= 1.10E+00

STEP	TIME	TB	D1	UR	ND	NC	NDROPS	D2
1	1.98E-04	1.98E-04	3.50E-02	4.70E+03	1.19E+01	1.59E+00	33	1.09E-02
2	2.81E-04	8.33E-05	1.09E-02	4.46E+03	3.42E+00	1.65E+00	9	5.25E-03
- -	EQUILIBRIUM - -		5.25E-03	4.46E+03	1.48E+00	1.74E+00		

TABLE B-2

BROWN AND YORK[5] CASE 1

INITIAL SIZE= 5.00E-02 INITIAL RELATIVE VELOCITY= 2.38E+03 GAS DENSITY= 2.01E-03 LIQUID DENSITY= 9.25E-01

SURFACE TENSION= 5.15E+01 KINEMATIC VISCOSITY= 2.10E-03 NCNU= 1.10E+00

STEP	TIME	TB	D1	UR	ND	NC	NDROPS	D2
1	6.99E-04	6.99E-04	5.00E-02	2.15E+03	1.11E+01	8.00E+00	17	1.94E-02
- -	EQUILIBRIUM - -		1.94E-02	2.15E+03	3.50E+00	8.00E+00		

TABLE B-3

SGTR CASES 1 AND 2

INITIAL SIZE= 1.00E-01 INITIAL RELATIVE VELOCITY= 1.00E+04 GAS DENSITY= 5.50E-02 LIQUID DENSITY= 6.90E-01

SURFACE TENSION= 1.15E+01 KINEMATIC VISCOSITY= 1.00E-03 NCNU= 1.10E+00

STEP	TIME	TB	D1	UR	ND	NC	NDROPS	D2
1	2.89E-05	2.89E-05	1.00E-01	7.43E+03	4.77E+04	1.84E+00	50	2.71E-02
2	3.95E-05	1.06E-05	2.71E-02	5.52E+03	7.15E+03	2.47E+00	50	7.37E-03
3	4.34E-05	3.87E-06	7.37E-03	4.10E+03	1.07E+03	3.33E+00	50	2.00E-03
4	4.48E-05	1.43E-06	2.00E-03	3.04E+03	1.60E+02	4.48E+00	50	5.43E-04
5	4.54E-05	5.99E-07	5.43E-04	2.17E+03	2.39E+01	6.05E+00	50	1.47E-04
- - EQUILIBRIUM - -			1.47E-04	2.17E+03	3.31E+00	8.00E+00		

INITIAL SIZE= 1.00E+00 INITIAL RELATIVE VELOCITY= 1.00E+04 GAS DENSITY= 5.50E-02 LIQUID DENSITY= 6.90E-01

SURFACE TENSION= 1.15E+01 KINEMATIC VISCOSITY= 1.00E-03 NCNU= 1.10E+00

STEP	TIME	TB	D1	UR	ND	NC	NDROPS	D2
1	2.89E-04	2.89E-04	1.00E+00	7.43E+03	4.77E+05	1.84E+00	50	2.71E-01
2	3.95E-04	1.06E-04	2.71E-01	5.52E+03	7.15E+04	2.47E+00	50	7.37E-02
3	4.33E-04	3.86E-05	7.37E-02	4.10E+03	1.07E+04	3.33E+00	50	2.00E-02
4	4.48E-04	1.41E-05	2.00E-02	3.05E+03	1.61E+03	4.48E+00	50	5.43E-03
5	4.53E-04	5.22E-06	5.43E-03	2.26E+03	2.41E+02	6.03E+00	50	1.47E-03
6	4.55E-04	2.14E-06	1.47E-03	1.62E+03	3.58E+01	8.00E+00	50	4.00E-04
- - EQUILIBRIUM - -			4.00E-04	1.62E+03	5.01E+00	8.00E+00		

APPENDIX C

SOLUTION METHOD FOR THE BOILING BREAKUP PROBLEM

The system of equations described in Sec. III-D for the boiling breakup model can be solved using Euler's method. For this we designate the time level for each variable with a superscript n so that the value of any quantity Q(t) is written Q^n for time $t = n\delta t$ where δt is the time increment. With this convention and the nomenclature of Sec. III-D we have the discrete system of equations

$$p^n = \left(\frac{T^n - 255.2}{117.8}\right)^{\frac{1}{0.223}} \times 10^6$$

$$c_{ps} = 9.5875 \times 10^6 (1. - T_e/647.3)^{-0.8566}$$

$$\rho_s^n = \frac{p^n}{(\gamma - 1)c_{ps}T^n} \qquad (\gamma = 1.3)$$

$$V_s^n = \frac{4}{3}\pi\left[(r^n)^3 - r_o^3\right]$$

$$M^n = \rho_s^n V_s^n$$

$$m_\ell^n = m_o - M^n$$

$$r^{n+1} = r^n + u^n \sigma t$$

$$A^n = 4\rho(r^n/2)^2$$

$$u^{n+1} = u^n + \frac{\delta t}{m_\ell^n}(p^n - p_e)A^n$$

$$T^{n+1} = T^n - \left(\frac{kA^n \delta t}{m_\ell^n c}\right)\left(\frac{T^n - T_e}{r^n}\right) - \frac{L}{m_\ell^n c}\left(\overline{\rho_s^{n+1}} V_s^{n+1} - m^n\right)$$

$$\overline{\rho_s^{n+1}} = \frac{\overline{p^{n+1}}}{(\gamma - 1)c_{ps}\overline{T^{n+1}}} \quad . \qquad \text{[C-1(a-k]}$$

The following FORTRAN program solves the system [C-1(a-k)]. Note that equations [C-1(j)] and [C-1(k)] require a Newton-Raphson iteration; the over-bar denotes values from the previous iteration.

```
      PROGRAM DBBRK(TTY,TAPE2=TTY,BOUT,TAPE1=BOUT)
      COMMON /DATA/ RO,TE,TO,DT,RS,T,R,P,TIME,
     1       K,C,L,GM1,CPS,PE,PO,ACC,NDROPS,RHOL
      REAL K,MN,ML,MO,L
      F1(T)=((T-255.2)/117.8)**(1./0.223)*1.E6
      READ(2,*) RO,TE,TO,DT,RHOL
      PE=F1(TE)
      P=F1(TO)
      WRITE(2,50) RO,TE,PE,TO,DT,RHOL,RHOG
   50 FORMAT(*  RO=*,1PE12.4,*  TE=*,1PE12.4,*  PE=*,1PE12.4/
     1  *  TO=*,1PE12.4,*  DT=*,1PE12.4,*  RHOL=*,1PE12.4,
     2  *  RHOG=*,1PE12.4)
      WRITE(1,100)
      WRITE(1,110) 2.*RO,TO,P,TE,PE,RHOL,DT
  100 FORMAT(39X,* - - - BOILING BREAKUP CALCULATION - - -*//)
  110 FORMAT(*   INITIAL SIZE = *,1PE8.2//
     1       *   INITIAL DROP TEMPERATURE = *,1PE8.2//
     #     *   INITIAL DROP PRESSURE = *,1PE8.2//
     2    *   EXTERIOR TEMPERATURE = *,1PE8.2//
     3    *   EXTERIOR PRESSURE = *,1PE8.2//
     4    *   LIQUID DENSITY = *,1PE8.2,*   TIME STEP = *,1PE8.2//)
      WRITE(1,120)
  120 FORMAT(2X,*STEP*,3X,*TIME*,10X,*D1*,10X,*T1*,9X,*ACC*,
     1   7X,*SIGMA*,6X,*NDROPS*,10X,*D2*,10X,*T2*/)
      TIME=0.
      L=2.3E10
      C=4.19E7
      K=6.2E4
      GM1=0.3
   10 CONTINUE
      T1=TO
      CALL BB(IEND)
      TO=T
      T2=T
      IF(IEND.EQ.0) THEN
      WRITE(2,45)
   45 FORMAT(*  BUBBLE IN THE DROP AT EQUILIBRIUM*)
      ENDIF
      D1=2.*RO
      IF(IEND.NE.0) THEN
      ITER=ITER+1
      SIGMA=70.9*(RHOL-RS)**4.
      RLM=6.28*SQRT(3.*SIGMA/(ACC*(RHOL-RS)))
      NDROPS=INT(12.57*(RO/RLM)**2.)
      NDROPS=MAXO(2,NDROPS)
      RO=RO/NDROPS**0.33333333
      D2=2.*RO
      WRITE(1,130) ITER,TIME,D1,T1,ACC,SIGMA,NDROPS,D2,T2
  130 FORMAT(I5,1P5E12.2,I6,6X,1P2E12.2)
      ENDIF
```

```
      IF(2.*SIGMA/RO+PE.LT.P) GOTO 10
      WRITE(2,40) RO,TIME,TO,NDROPS
   40 FORMAT(*  RO=*,1PE12.4,
     1   *  TIME=*,1PE12.4,*  TO=*,1PE12.4,*  NDROPS=*,I4)
  200 WRITE(1,140) 2.*R , T-TE
  140 FORMAT(/*      - - - EQUILIBRIUM SIZE = *,1PE8.2,* - - -*,
     1   *  - - - EQUILIBRIUM SUPERHEAT = *,1PE9.2,* - - -*//)
      STOP
      END
      SUBROUTINE BB(IEND)
      COMMON /DATA/ RO,TE,TO,DT,RS,T,R,P,TIME,
     1       K,C,L,GM1,CPS,PE,PO,ACC,NDROPS,RHOL
      REAL K,MN,ML MO,L
      F1(T)=((T-255.2)/117.8)**(1./0.223)*1.E6
      F2(P,T,GM1,CPS)=P/(GM1*CPS*T)
      F3(R,RO)=4.19*(R**3.-RO**3.)
      F4(R)=12.57*(R/2.)**2.
      PO=F1(TO)
      WRITE(2,40) RO,TIME,TO,NDROPS
      MO=4.19*RO**3.
      VO=MO
      U=0.
      T=TO
      TN=T
      R=RO
      V=VO
      P=PO
C  10 WRITE(2,35) TIME,V,R,P,T
      NDT=0
      ACC=0.
   10 CONTINUE
      IEND=0
      P=F1(T)
      CPS=9.5857E6*(1.-T/647.3)**(-0.8566)
      RS=F2(P,T,GM1,CPS)
      SIGMA=70.9*(RHOL-RS)**4.
      IF(2.*SIGMA/R+PE.GT.P) THEN
      ACC=ACC/NDT
      RETURN
      ENDIF
      IEND=1
      V=F3(R,RO)
      MN=RS*V
      ML=MO-MN
      A=F4(R)
      R=R+U*DT
      V=F3(R,RO)
      U=U+DT/ML*(P-PE-2.*SIGMA/R)*A
      ACC=(P-PE+2.*SIGMA/R)*A/ML+ACC
      N=0
   20 F=T-TN+K*A*DT/(ML*C)*(T-TE)/R+L*(RS*V-MN)/(ML*C)
      DFDT=1.+L*V/(ML*C*GM1*CPS)*(3.81E4/T*((T-255.2)/117.8)**3.48
     1    -F1(T)/(1+T))+K*A*DT/(ML*C*R)
      T=T-F/DFDT
      P=F1(T)
      RS=F2(P,T,GM1,CPS)
      N=N+1
      IF(N.GT.20) PAUSE
      IF(ABS(F/DFDT/T).GT.1.E-4) GOTO 20
      TN=T
      TIME=TIME+DT
      NDT=NDT+1
      IF(V.LT.2.*VO) GOTO 10
      ACC=ACC/NDT
      WRITE(2,35) V,P,T,U,ACC
   30 FORMAT(*  N=*,I3,*  P=*,1PE12.4,*  T=*,1PE12.4)
   35 FORMAT(* V,P,T,U,ACC=*,1P5E12.4)
   40 FORMAT(*  RO=*,1PE12.4,
     1   *  TIME=*,1PE12.4,*  TO=*,1PE12.4,*  NDROPS=*,I4)
      RETURN
      END
```

Tables C-1 through C-4 list the results of the calculations for the Brown and York[5] and Alger and Geidt[2] experimental conditions. Tables C-5 through C-7 give results for the three sets of SGTR conditions considered. In these tables, units are cgsK, D1 and D2 are the beginning and ending drop sizes for each step of the cascade process, T1 and T2 are the beginning and ending drop temperatures for each step, ACC is the acceleration, SIGMA is the surface tension and NDROPS is the number of drops produced at each cascade step. Note that in the cases of Brown and York, and Alger and Geidt conditions that the equilibrium is approached slowly leaving a positive droplet superheat. In the cases of SGTR conditions, the equilibrium is approached in just a few cascade steps, with a large number of drops for each step, leaving essentially no superheat in the droplet temperature. This reflects the violence with which boiling breakup occurs at SGTR temperatures which is partly due to the small surface tension compared to the lower temperature cases for which there are experimental data.

TABLE C-1

BROWN AND YORK[5] CASE 1

INITIAL SIZE = 1.00E-02

INITIAL DROP TEMPERATURE = 4.14E+02

INITIAL DROP PRESSURE = 3.82E+06

EXTERIOR TEMPERATURE = 3.73E+02

EXTERIOR PRESSURE = 1.00E+06

LIQUID DENSITY = 9.25E-01 TIME STEP = 5.00E-09

STEP	TIME	D1	T1	ACC	SIGMA	NDROPS	D2	T2
1	3.05E-06	1.00E-02	4.14E+02	5.50E+08	5.16E+01	26	3.38E-03	4.13E+02
2	4.12E-06	3.38E-03	4.13E+02	1.56E+09	5.16E+01	8	1.69E-03	4.11E+02
3	4.68E-06	1.69E-03	4.11E+02	3.01E+09	5.16E+01	4	1.06E-03	4.10E+02
4	5.05E-06	1.06E-03	4.10E+02	4.63E+09	5.16E+01	2	8.44E-04	4.08E+02
5	5.36E-06	8.44E-04	4.08E+02	5.65E+09	5.16E+01	2	6.70E-04	4.07E+02
6	5.62E-06	6.70E-04	4.07E+02	6.90E+09	5.17E+01	2	5.32E-04	4.06E+02
7	5.84E-06	5.32E-04	4.06E+02	8.49E+09	5.17E+01	2	4.22E-04	4.04E+02
8	6.02E-06	4.22E-04	4.04E+02	1.04E+10	5.17E+01	2	3.35E-04	4.03E+02
9	6.19E-06	3.35E-04	4.03E+02	1.32E+10	5.17E+01	2	2.66E-04	4.02E+02
10	6.34E-06	2.66E-04	4.02E+02	1.68E+10	5.17E+01	2	2.11E-04	4.00E+02
11	6.48E-06	2.11E-04	4.00E+02	2.15E+10	5.17E+01	2	1.67E-04	3.99E+02
12	6.67E-06	1.67E-04	3.99E+02	2.78E+10	5.17E+01	2	1.33E-04	3.97E+02

- - - EQUILIBRIUM SIZE = 2.43E-04 - - - - - - EQUILIBRIUM SUPERHEAT = 2.38E+01 - - -

TABLE C-2

BROWN AND YORK[5] CASE 2

INITIAL SIZE = 5.00E-02

INITIAL DROP TEMPERATURE = 4.14E+02

INITIAL DROP PRESSURE = 3.82E+06

EXTERIOR TEMPERATURE = 3.73E+02

EXTERIOR PRESSURE = 1.00E+06

LIQUID DENSITY = 9.25E-01 TIME STEP = 5.00E-09

STEP	TIME	D1	T1	ACC	SIGMA	NDROPS	D2	T2
1	1.52E-05	5.00E-02	4.14E+02	1.09E+08	5.16E+01	129	9.90E-03	4.13E+02
2	1.83E-05	9.90E-03	4.13E+02	5.26E+08	5.16E+01	24	3.43E-03	4.11E+02
3	1.94E-05	3.43E-03	4.11E+02	1.46E+09	5.16E+01	8	1.72E-03	4.10E+02
4	2.00E-05	1.72E-03	4.10E+02	2.81E+09	5.16E+01	3	1.19E-03	4.08E+02
5	2.04E-05	1.19E-03	4.08E+02	3.92E+09	5.16E+01	2	9.44E-04	4.07E+02
6	2.08E-05	9.44E-04	4.07E+02	4.77E+09	5.17E+01	2	7.49E-04	4.06E+02
7	2.11E-05	7.49E-04	4.06E+02	5.80E+09	5.17E+01	2	5.95E-04	4.05E+02
8	2.13E-05	5.95E-04	4.05E+02	7.15E+09	5.17E+01	2	4.72E-04	4.03E+02
9	2.15E-05	4.72E-04	4.03E+02	8.79E+09	5.17E+01	2	3.75E-01	4.02E+02
10	2.17E-05	3.75E-04	4.02E+02	1.11E+10	5.17E+01	2	2.97E-04	4.01E+02
11	2.19E-05	2.97E-04	4.01E+02	1.40E+10	5.17E+01	2	2.36E-04	3.99E+02
12	2.20E-05	2.30E-04	3.99E+02	1.81E+10	5.17E+01	2	1.87E-04	3.98E+02
13	2.22E-05	1.6[illegible]-04	3.98E+02	2.32E+10	5.17E+01	2	1.49E-01	3.96E+02

- - - EQUILIBRIUM SIZE = 2.71E-04 - - - - - - EQUILIBRIUM SUPERHEAT = 2.32E+01 - - -

TABLE C-3

ALGER AND GEIDT[2] CASE 1

INITIAL SIZE = 6.00E-02

INITIAL DROP TEMPERATURE = 4.43E+02

INITIAL DROP PRESSURE = 8.10E+06

EXTERIOR TEMPERATURE = 3.77E+02

EXTERIOR PRESSURE = 1.16E+06

LIQUID DENSITY = 8.98E-01 TIME STEP = 5.00E-09

STEP	TIME	D1	T1	ACC	SIGMA	NDROPS	D2	T2
1	1.16E-05	6.00E-02	4.43E+02	2.23E+08	4.56E+01	419	8.02E-03	4.41E+02
2	1.32E-05	8.02E-03	4.41E+02	1.56E+09	4.57E+01	52	2.15E-03	4.39E+02
3	1.37E-05	2.15E-03	4.38E+02	5.48E+09	4.57E+01	13	9.14E-04	4.36E+02
4	1.39E-05	9.14E-04	4.36E+02	1.22E+10	4.57E+01	5	5.34E-01	4.33E+02
5	1.40E-05	[illegible]4E-04	4.33E+02	2.00E+10	4.57E+01	2	4.24E-04	4.31E+02
6	1.41E-05	[illegible]E-04	4.31E+02	2.38E+10	4.57E+01	2	3.37E-04	4.29E+02
7	1.42E-0[illegible]	[illegible]E-04	4.29E+02	2.79E+10	4.57E+01	2	2.67E-04	4.27E+02
8	1.43E-05	[illegible].67E-04	4.27E+02	3.45E+10	4.58E+01	2	2.12E-04	4.24E+02
9	1.44E-05	2.12E-04	4.24E+02	4.18E+10	4.58E+01	2	1.68E-04	4.22E+02
10	1.44E-05	1.68E-04	4.22E+02	5.01E+10	4.58E+01	2	1.34E-04	4.19E+02
11	1.45E-05	1.34E-04	4.19E+02	6.24E+10	4.58E+01	2	1.06E-04	4.17E+02
12	1.45E-05	1.06E-04	4.17E+02	7.96E+10	4.58E+01	2	8.41E-05	4.14E+02
13	1.46E-05	8.41E-05	4.14E+02	1.00E+11	4.59E+01	2	6.68E-05	4.11E+02

- - - EQUILIBRIUM SIZE = 1.27E-04 - - - - - - EQUILIBRIUM SUPERHEAT = 3.37E+01 - - -

TABLE C-4

ALGER AND GEIDT[2] CASE 2

INITIAL SIZE = 1.00E-01

INITIAL DROP TEMPERATURE = 4.43E+02

INITIAL DROP PRESSURE = 8.10E+06

EXTERIOR TEMPERATURE = 3.77E+02

EXTERIOR PRESSURE = 1.16E+06

LIQUID DENSITY = 8.98E-01 TIME STEP = 5.00E-09

STEP	TIME	D1	T1	ACC	SIGMA	NDROPS	D2	T2
1	1.93E-05	1.00E-01	4.43E+02	1.34E+08	4.56E+01	698	1.13E-02	4.41E+02
2	2.16E-05	1.13E-02	4.41E+02	1.11E+09	4.57E+01	73	2.70E-03	4.38E+02
3	2.22E-05	2.70E-03	4.38E+02	4.37E+09	4.57E+01	16	1.07E-03	4.36E+02
4	2.24E-05	1.07E-03	4.36E+02	1.04E+10	4.57E+01	6	5.89E-04	4.33E+02
5	2.26E-05	5.89E-04	4.33E+02	1.79E+10	4.57E+01	3	4.08E-04	4.31E+02
6	2.27E-05	4.08E-04	4.31E+02	2.47E+10	4.57E+01	2	3.24E-04	4.29E+02
7	2.28E-05	3.24E-04	4.29E+02	2.97E+10	4.58E+01	2	2.57E-04	4.26E+02
8	2.28E-05	2.57E-04	4.26E+02	3.52E+10	4.58E+01	2	2.04E-04	4.24E+02
9	2.29E-05	2.04E-04	4.24E+02	4.29E+10	4.58E+01	2	1.62E-04	4.22E+02
10	2.30E-05	1.62E-04	4.22E+02	5.39E+10	4.58E+01	2	1.29E-04	4.19E+02
11	2.30E-05	1.29E-04	4.19E+02	6.63E+10	4.58E+01	2	1.02E-04	4.17E+02
12	2.31E-05	1.02E-04	4.17E+02	8.36E+10	4.58E+01	2	8.10E-05	4.14E+02
13	2.31E-05	8.10E-05	4.14E+02	1.05E+11	4.59E+01	2	6.43E-05	4.10E+02

- - - EQUILIBRIUM SIZE = 1.23E-04 - - - - - - EQUILIBRIUM SUPERHEAT = 3.33E+01 - - -

TABLE C-5

SGTR CASE 1 AND 2

INITIAL SIZE = 1.00E-01

INITIAL DROP TEMPERATURE = 5.90E+02

INITIAL DROP PRESSURE = 1.08E+08

EXTERIOR TEMPERATURE = 5.60E+02

EXTERIOR PRESSURE = 7.10E+07

LIQUID DENSITY = 6.99E-01 TIME STEP = 5.00E-09

STEP	TIME	D1	T1	ACC	SIGMA	NDROPS	D2	T2
1	8.51E-06	1.00E-01	5.90E+02	6.58E+08	1.62E+01	7480	5.11E-03	5.82E+02
2	9.04E-06	5.11E-03	5.82E+02	8.41E+09	1.62E+01	249	8.13E-04	5.73E+02
3	9.16E-06	8.13E-04	5.73E+02	2.72E+10	1.62E+01	20	2.99E-04	5.64E+02

- - - EQUILIBRIUM SIZE = 3.71E-04 - - - - - - EQUILIBRIUM SUPERHEAT = 4.41E-02 - - -

INITIAL SIZE = 1.00E+00

INITIAL DROP TEMPERATURE = 5.30E+02

INITIAL DROP PRESSURE = 1.08E+08

EXTERIOR TEMPERATURE = 5.60E+02

EXTERIOR PRESSURE = 7.10E+07

LIQUID DENSITY = 6.99E-01 TIME STEP = 5.00E-09

STEP	TIME	D1	T1	ACC	SIGMA	NDROPS	D2	T2
1	8.51E-05	1.00E+00	5.90E+02	6.59E+07	1.62E+01	74816	2.37E-02	5.82E+02
2	8.75E-05	2.37E-02	5.82E+02	1.81E+09	1.62E+01	1160	2.26E-03	5.73E+02
3	8.78E-05	2.26E-03	5.73E+02	9.80E+09	1.62E+01	56	5.90E-04	5.64E+02

- - - EQUILIBRIUM SIZE = 7.53E-04 - - - - - - EQUILIBRIUM SUPERHEAT = -1.36E-01 - - -

TABLE C-6

SGTR CASE 3 AND 4

INITIAL SIZE = 1.00E-01

INITIAL DROP TEMPERATURE = 5.80E+02

INITIAL DROP PRESSURE = 9.45E+07

EXTERIOR TEMPERATURE = 5.60E+02

EXTERIOR PRESSURE = 7.10E+07

LIQUID DENSITY = 6.99E-01 TIME STEP = 5.00E-09

STEP	TIME	D1	T1	ACC	SIGMA	NDROPS	D2	T2
1	1.08E-05	1.00E-01	5.80E+02	3.92E+08	1.62E+01	4453	6.08E-03	5.71E+02
2	1.18E-05	6.08E-03	5.71E+02	3.06E+09	1.62E+01	128	1.21E-03	5.63E+02

- - - EQUILIBRIUM SIZE = 1.43E-03 - - - - - - EQUILIBRIUM SUPERHEAT = -3.47E-02 - - -

INITIAL SIZE = 1.00E+00

INITIAL DROP TEMPERATURE = 5.80E+02

INITIAL DROP PRESSURE = 9.45E+07

EXTERIOR TEMPERATURE = 5.60E+02

EXTERIOR PRESSURE = 7.10E+07

LIQUID DENSITY = 6.99E-01 TIME STEP = 5.00E-09

STEP	TIME	D1	T1	ACC	SIGMA	NDROPS	D2	T2
1	1.08E-04	1.00E+00	5.80E+02	3.92E+07	1.62E+01	44536	2.82E-02	5.71E+02
2	1.13E-04	2.82E-02	5.71E+02	6.59E+08	1.62E+01	595	3.35E-03	5.63E+02

- - - EQUILIBRIUM SIZE = 4.00E-03 - - - - - - EQUILIBRIUM SUPERHEAT = -1.12E-02 - - -

TABLE C-7

SGTR CASE 5 AND 6

INITIAL SIZE = 1.00E-01

INITIAL DROP TEMPERATURE = 5.62E+02

INITIAL DROP PRESSURE = 7.31E+07

EXTERIOR TEMPERATURE = 5.60E+02

EXTERIOR PRESSURE = 7.10E+07

LIQUID DENSITY = 6.99E-01 TIME STEP = 5.00E-09

STEP	TIME	D1	T1	ACC	SIGMA	NDROPS	D2	T2

- - - EQUILIBRIUM SIZE = 1.00E-01 - - - - - - EQUILIBRIUM SUPERHEAT = -8.94E-05 - - -

INITIAL SIZE = 1.00E+00

INITIAL DROP TEMPERATURE = 5.62E+02

INITIAL DROP PRESSURE = 7.31E+07

EXTERIOR TEMPERATURE = 5.60E+02

EXTERIOR PRESSURE = 7.10E+07

LIQUID DENSITY = 6.99E-01 TIME STEP = 5.00E-09

STEP	TIME	D1	T1	ACC	SIGMA	NDROPS	D2	T2

- - - EQUILIBRIUM SIZE = 1.00E+00 - - - - - - EQUILIBRIUM SUPERHEAT = -1.02E-04 - - -

APPENDIX D

SOLUTION METHOD FOR THE DUAL STREAM DISCHARGE PROBLEM

Consider two reservoirs A and B discharging through pipes of length L_a and L_b from pressures p_{o_a} and p_{o_b} both to pressure p_o. Across the exit there must be a single pressure drop $(p_e - p_o)$ and a single exit impedance, implying a single velocity. What are u_a and u_b, the velocities in each pipe? We can write

$$(p_{o_a} - p_e) = \left(K_{1a} + f\frac{L_a}{D}\right)\frac{1}{2}\rho_o u_a^2$$

$$(p_{o_b} - p_e) = \left(K_{1b} + f\frac{L_b}{D}\right)\frac{1}{2}\rho_o u_b^2$$

$$(u_a + u_b)A = u_e A_e$$

$$(p_e - p_o) = K_2\frac{1}{2}\rho_o(u_e)^2 \quad , \qquad \text{[D-1(a-d)]}$$

where K_{1a} and K_{1b} are the entrance loss coefficients for pipes a and b respectively, A is the flow area of pipes a and b (which are the same size), A_e is the flow area of the exit and u_e is the discharge velocity at the exit. These continue to give

$$u_a^2 = \frac{\left[p_a - \left(p_o + K_2\frac{1}{2}\rho_o(u_a + u_b)^2\left(\frac{A}{A_{out}}\right)^2\right)\right]}{K_{1a} + f\frac{L_b}{D}\ \frac{i}{2}\rho_o}$$

$$u_b^2 = \frac{\left[p_b - \left(p_o + K_2\frac{1}{2}\rho_o(u_a + u_b)^2\left(\frac{A}{A_{out}}\right)^2\right)\right]}{K_{1b} + f\frac{L_b}{D}\ \frac{i}{2}\rho_o}$$

which can be rearranged as

$$u_a^2(1 + C_{1a}) + 2C_{1a}u_a u_b + C_{1a}u_b^2 - C_{2a} = 0$$

$$u_b^2(1 + C_{1b}) + 2C_{1b}u_a u_b + C_{1b}u_a^2 - C_{2b} = 0 \qquad \text{[D-2(a-b)]}$$

where

$$C_{1a} = \frac{p_o + K_2 \frac{1}{2}\rho_o \left(\frac{A}{A_e}\right)^2}{\left(K_{1a} + f\frac{L_a}{D}\right)\frac{1}{2}\rho_o}$$

$$C_{2a} = \frac{p_a}{\left(K_{1a} + f\frac{L_a}{D}\right)\frac{1}{2}\rho_o}$$

$$C_{1b} = \frac{p_o + K_2 \frac{1}{2}\rho_o \left(\frac{A}{A_e}\right)^2}{\left(K_{1b} + f\frac{L_b}{D}\right)\frac{1}{2}\rho_o}$$

$$C_{2b} = \frac{p_b}{\left(K_{1b} + f\frac{L_b}{D}\right)\frac{1}{2}\rho_o} \quad .$$

Equations [D-2(a-b)] can be solved iteratively using a Newton-Raphson technique as follows. First set the right-hand side of Eqs. [D-2(a-b)] equal to F_1 and F_2 respectively. Then, designating iterate levels with a superscript k, compute successive estimates for u_a and u_b using

$$u_a^{k+1} = u_a^k - \frac{\left[-F_1^k \frac{\partial F_2}{\partial u_b} + F_2^k \frac{\partial F_1}{\partial u_b}\right]}{\left[\frac{\partial F_1}{\partial u_a}\frac{\partial F_2}{\partial u_b} - \frac{\partial F_1}{\partial u_b}\frac{\partial F_2}{\partial u_a}\right]}$$

$$u_b^{k+1} = u_b^k - \frac{\left[- F_2^k \frac{\partial F_1}{\partial u_a} + F_1^k \frac{\partial F_2}{\partial u_a} \right]}{\left[\frac{\partial F_1}{\partial u_a} \frac{\partial F_2}{\partial u_b} - \frac{\partial F_1}{\partial u_b} \frac{\partial F_2}{\partial u_a} \right]}$$

where the derivatives

$$\frac{\partial F_1}{\partial u_a} = 2u_a(1 + C_{1a}) + 2C_{1a}u_b$$

$$\frac{\partial F_1}{\partial u_b} = 2C_{1a}u_a + 2C_{1a}u_b$$

$$\frac{\partial F_2}{\partial u_a} = 2C_{1b}u_b + 2C_{1b}u_a$$

$$\frac{\partial F_2}{\partial u_b} = 2u_b(1 + C_{1b}) + 2C_{1b}u_a$$

are all defined at the level k. This can be repeated until a suitably stationary solution is obtained.

REFERENCES

1. L. G. Alexander and C. L. Coldren, "Droplet Transfer from Suspending Air to Duct Walls," Ind. Eng. Chem., 43, pp. 1325-1331 (1951).

2. T. W. Alger and W. H. Geidt, "A Light Scattering Technique for Determining Droplet Size Distributions in Two-Phase Liquid-Dominated Nozzle Jets," Proceedings of the First International Conference on Liquid Atomization and Spray Systems, Tokyo, Japan, Aug., 1978.

3. S. G. Bankoff, "Steam Generator Leak Project," Northwestern University, document in preparation for U.S. Nuclear Regulatory Commission.

4. T. Baumeister and L. S. Marks, eds, Standard Handbook for Mechanical Engineers, McGraw-Hill, N.Y., 7th ed., pp. 3-69 (1967).

5. R. Brown and J. L. York, "Sprays Formed by Flashing Liquid Jets," AIChE J., 8, pp. 149-153 (1962).

6. R. Brown, "Sprays Formed by Flashing Liquid Jets," University of Michigan Doctoral Dissertation, 1960.

7. G. P. Celata, M. Cumo, G. E. Farello, P. C. Incalcaterra, and R. Centi, "Critical Flow Jets Investigation for Engineering Application," in Multiphase Flow and Heat Transfer, T. Nejat Zeziroglu, Ed. (Elsevier Publishing, New York, 1984).

8. G. P. Celata, M. Cumo, G. E. Farello, P. C. Incalcaterra, and A. Naviglio, "Thermodynamic Disequilibrium in the Critical Flow of Subcooled Liquids," Nuclear Technology, 60, pp. 137-142 (1983).

9. C. F. Chuang, "Consequence Analysis for a Steam Generator Tube Rupture Accident," Doctoral Thesis, Rensselaer Polytechnic Institute, Troy NY (1983).

10. R. Cole, "Boiling Nucleation," Adv. in Heat Transfer, 10, pp. 86-166 (1974).

11. W. J. Comfort III and C. T. Crowe, "Dependence of Shock Characteristics on Droplet Size in Supersonic Two-Phase Mixtures," Trans ASME, J. Fluids Eng., 102, pp. 54-58 (1980).

12. C. T. Crowe and W. J. Comfort, III, "Atomization Mechanisms in Single-Component, Two-Phase, Nozzle Flows," Proceedings of the First International Conference on Liquid Atomization and Spray Systems (The Fuel Society of Japan, Tokyo, 1979), p. 45.

13. D. Dobranich, "Steam Generator Tube Rupture Analysis for Zion-1," Los Alamos National Laboratory document LA-SSTS-TN-81-2 (1981).

14. D. Dobranich, "Steam Generator Tube Rupture Analysis for TMI-1," Los Alamos National Laboratory document LA-SSTS-TN-81-1 (1981).

15. D. Dobranich, R. J. Henninger, and N. S. Demuth, "Steam-Generator-Tube-Rupture Transients for Pressurized Water Reactors," Los Alamos National Laboratory document LA-UR-82-2498, presented at the International Meeting on Nuclear Reactor Safety, Aug. 29-Sept. 2, 1982, Chicago.

16. N. Dombrowski and P. C. Hooper, "The Effect of Ambient Density on Drop formation in Sprays," Chem. Eng. Sci., 17, pp. 291-305 (1962).

17. W. Frid, "Jet Behavior in High Pressure Melt Ejection from a Reactor Pressure Vessel--Part I, Jet Expansion Due to Effervescence of Gas Dissolved in the Melt," Sandia National Laboratory, document in preparation.

18. R. J. Henninger, "Steam Generator Tube Rupture Analysis for Calvert Cliffs-1," Los Alamos National Laboratory document LA-SSTS-TN-81-3 (1981).

19. R. E. Henry and H. K. Fauske, "The Two-Phase Critical Flow of One-Component Mixtures in Nozzles, Orifices, and Short Tubes," Trans. ASME, J. Heat Transfer 95, pp. 179-187 (1971).

20. J. O. Hinze, "Critical Speeds and Sizes of Liquid Globules," Appl. Sci. Res., A1, pp. 273-288 (1948).

21. J. O. Hinze, "Forced Deformations of Viscous Liquid Globules," Appl. Sci. Res., A1, pp. 263-272 (1948).

22. J. O. Hinze, "Fundamentals of the Hydrodynamic Mechanism of Splitting in Dispersion Processes," AIChE Journal, 1, pp. 289-295 (1955).

23. J. Hopenfeld, "Radioactivity Transfer Following Steam Generator Tube Rupture," U.S. Nuclear Regulatory Commission, document in preparation.

24. M. Ishii, "Wave Phenomena and Two-Phase Flow Instabilities," Ch. 2.4 in G. Hetsroni, ed., Handbook of Multiphase Systems, Hemisphere, Washington (1982).

25. O. C. Jones, Jr., "Flashing Inception in Flowing Liquids," Trans. ASME, J. Heat Transfer, 102, pp. 439-444 (1980).

26. B. A. Kashiwa, F. H. Harlow, R. B. Demuth, and H. M. Ruppel, "Steam-Water Jet Analysis," EPRI Research Project RP-1324-4, Final Report, May, 1984.

27. W. R. Lane, "Shatter of Drops in Streams of Air," Ind. Eng. Chem., 43, pp. 1312-1317 (1951).

28. J. H. Lienhard and J. B. Day, "The Breakup of Superheated Liquid Jets," Trans. ASME, J. Basic Engineering 90, pp. 515-522 (1970).

29. J. H. Lienhard and J. M. Stephenson, "Temperature and Scale Effects Upon Cavitation in Free and Submerged Jets," Trans. ASME, J. Basic Eng., 88, pp. 525-532 (1966).

30. J. M. McKelliget, M. Cross, and R. D. Gibson, "Limitations of Existing Models Describing Submerged Gas Jets," Ironmaking and Steelmaking, No. 6, pp. 282-284 (1978).

31. G. Morrell, "Breakup of Liquid Jets by Transverse Shocks," in 8th Symposium (International) on Combustion held at California Inst. Tech., 1960. Proceedings published by Williams and Wilkins Co., Baltimore, 1982.

32. R. A. Mugele and H. D. Evans, "Droplet Size Distribution in Sprays," Ind. Eng. Chem., 43, pp. 1317-1324 (1951).

33. S. Nagaosa, H. Matsui, N. Tokuoka, and G. T. Sato, "A Study of the Disintegration of a Liquid Jet in an Air Flow," Proceedings of the First International Conference on Liquid Atomization and Spray Systems (The Fuel Society of Japan, Tokyo, 1979), p. 29.

34. B. Nassersharif, "Combined Steam-Generator-Tube-Rupture and Loss-of-Feedwater Transients for the Zion-1 PWR," Los Alamos National Laboratory document LA-UR-83-3251, 1983.

35. Nuclear Regulatory Commission, Office of Nuclear Reactor Regulation, "Safety Evaluations Report Related to Restart of R. E. Ginna Nuclear Power Plant," NUREG 0916, May 1982.

36. G. N. Oryall and J. K. Brimacombe, "The Physical Behavior of a Gas Jet Injected Horizontally into a Liquid Metal," Metallurgical Transactions B, 7B, pp. 391-403 (1976).

37. H. S. Ostrowski, "Evaporation and Induced Air Flow in Sprays Produced by Superheated Water Jets," University of Michigan Doctoral Dissertation, 1966.

38. K. L. Peddicord, "Assessment of the Effect of Critical Flow and Critical Heat Flux Models on Super Sara Thermal Hydraulic Analysis," Commission of the European Communities Joint Research Centre Technical Note No. 1.06.19.83.18, February 1983.

39. S. Raghuram, P. Baybutt, R. S. Denning, and H. Jordan "Iodine Behavior in Steam Generator Tube Rupture Accidents," Battelle Columbus Laboratories report NUREG/CR-2683, BMI-2094 (1982).

40. W. C. Rivard and J. R. Travis, "A Nonequilibrium Vapor Production Model for Critical Flow," Los Alamos National Laboratory document LA-UR-79-1058 (p. 8) 1979.

41. P. Saha, "A Review of Two-Phase Steam-Water Critical Flow Models with Emphasis on Thermal Nonequilibrium," Brookhaven National Laboratory Report BNL-NUREG-50909 (also NUREG/CR-0417)(1978).

42. P. Saha, N. Abauf, and B. J. C. Wu, "A Nonequilibrium Vapor Generation Model for Flashing Flows," ASME paper 81-HT-84, presented at the 20th joint ASME/AICHE National Heat Transfer Conference, Milwaukee, Wisconsin, Aug. 2-5, 1981.

43. V. E. Schrock, E. S. Starkman, and R. A. Brown, "Flashing Flow of Initially Subcooled Water in Convergent-Divergent Nozzles," Trans. ASME, J. Heat Transfer, 99, pp. 263-268 (1977).

44. W. L. Short, "Some Properties of Sprays Formed by the Disintegration of a Superheated Liquid Jet," University of Michigan Doctoral Dissertation, 1963.

45. T. G. Simpkins, "Non-Linear Effects on Droplet Deformation," Proceedings of the International Colloquium on Drops and Bubbles, Aug., 1974, Calif. Inst. Tech., Vol. II, pp. 372-309.

46. V. P. Skripov, Metastable Liquids, John Wiley & Sons, N.Y. (1974).

47. C. A. Sleicher and M. Tribus, "Heat Transfer in a Pipe with Turbulent Flow and Arbitary Wall-Temperature Distribution," Heat Transfer and Fluid Mechanics Institute, Stanford University Press, Stanford, Calif. (1981), p. 59.

48. G. L. Sozzi and W. A. Sutherland, "Critical Flow of Saturated and Subcooled Water at High Pressure," General Electric report NEDO-13418, July 1978.

49. V. L. Streeter, Ed., Handbook of Fluid Dynamics, McGraw-Hill, New York (1961) pp. 3-18 to 3-23.

50. M. Suzuki, T. Yamamoto, N. Futagami, and S. Maeda, "Atomization of Superheated Liquid Jets," Proceedings of the First International Conference on Liquid Atomization and Spray Systems (The Fuel Society of Japan, Tokyo, 1979), p. 37.

51. N. J. Themelis, P. Tarassoff, and J. Szekely, "Gas-Liquid Momentum Transfer in a Copper Converter," Trans. Metallurgical Society of AIME, 245, pp. 2425-2433 (1969).

52. Y. Tsuji and Y. Morikawa, "LDV Measurements of an Air-Solid Two-Phase Flow in a Horizontal Pipe," J. Fluid Mech. 120, pp 385-409 (1982).

53. A. M. Worthington, A Study of Splashes, The MacMillan Company, New York (1963).

54. M. Y. Young, K. Takeuchi, O. J. Mendler, and G. W. Hopkins, "Prototypical Steam Generator (MB-2) Transient Testing Program," Westinghouse Electric Corp. Report WCAP 10475 (also NUREG/CR-3661 and EPRI NP-3494)(1984).

55. "Zion Station Final Safety Analysis Report," Commonwealth Edison Company (1973).

DISTRIBUTION

	Copies
Nuclear Regulatory Commission, R4, Bethesda, Maryland	298
Technical Information Center, Oak Ridge, Tennessee	2
Los Alamos National Laboratory, Los Alamos, New Mexico	50
	350

NRC FORM 335 (6-83) U.S. NUCLEAR REGULATORY COMMISSION

BIBLIOGRAPHIC DATA SHEET

1 REPORT NUMBER (Assigned by TIDC, add Vol. No., if any)
NUREG/CR-4079
LA-10307-MS

2 Leave blank

3 TITLE AND SUBTITLE
Analytic Studies Pertaining to Steam Generator Tube Rupture Accidents

4 RECIPIENT'S ACCESSION NUMBER

5 DATE REPORT COMPLETED
MONTH: December YEAR: 1984

6 AUTHOR(S)
B. A. Kashiwa and R. C. Mjolsness

7 DATE REPORT ISSUED
MONTH: March YEAR: 1985

8 PERFORMING ORGANIZATION NAME AND MAILING ADDRESS (Include Zip Code)
Los Alamos National Laboratory
Los Alamos, NM 87545

9 PROJECT/TASK/WORK UNIT NUMBER

10 FIN NUMBER
A7247

11 SPONSORING ORGANIZATION NAME AND MAILING ADDRESS (Include Zip Code)
Division of Accident Evaluation
Office of Nuclea Regulatory Research
US Nuclear Regu ory Commission
Washington, DC 55

12a TYPE OF REPORT
Informal

12b PERIOD COVERED (Inclusive dates)

13 SUPPLEMENTARY NOTES

14 ABSTRACT (200 words or less)

A study of the thermal-hydraulic phenomena of possible steam generator tube rupture (SGTR) accidents leads to the conclusions that (1) flashing will not occur upstream of the tube rupture, so that the flow will be resistance limited rather than choked, (2) there is considerable potential for discharging the primary fluid in the form of micron-sized droplets, particularly when the fluid discharges into a vapor cavity surrounding the tube rupture, and (3) that the surrounding of the rupture site by water rather than vapor may be a means for preventing the formation of micron-sized droplets. The presence or absence of micron-sized droplets is considered to be a key issue for the damage assessment of SGTR accidents because they are currently thought to be the most likely route for radioactive iodine to be released to the atmosphere.

15a KEY WORDS AND DOCUMENT ANALYSIS

15b DESCRIPTORS

16 AVAILABILITY STATEMENT
Unlimited

17 SECURITY CLASSIFICATION (This report)
Unclassified

18 NUMBER OF PAGES

19 SECURITY CLASSIFICATION (This page)
Unclassified

20 PRICE
$

☆ U.S. GOVERNMENT PRINTING OFFICE 1985—576-034/20039

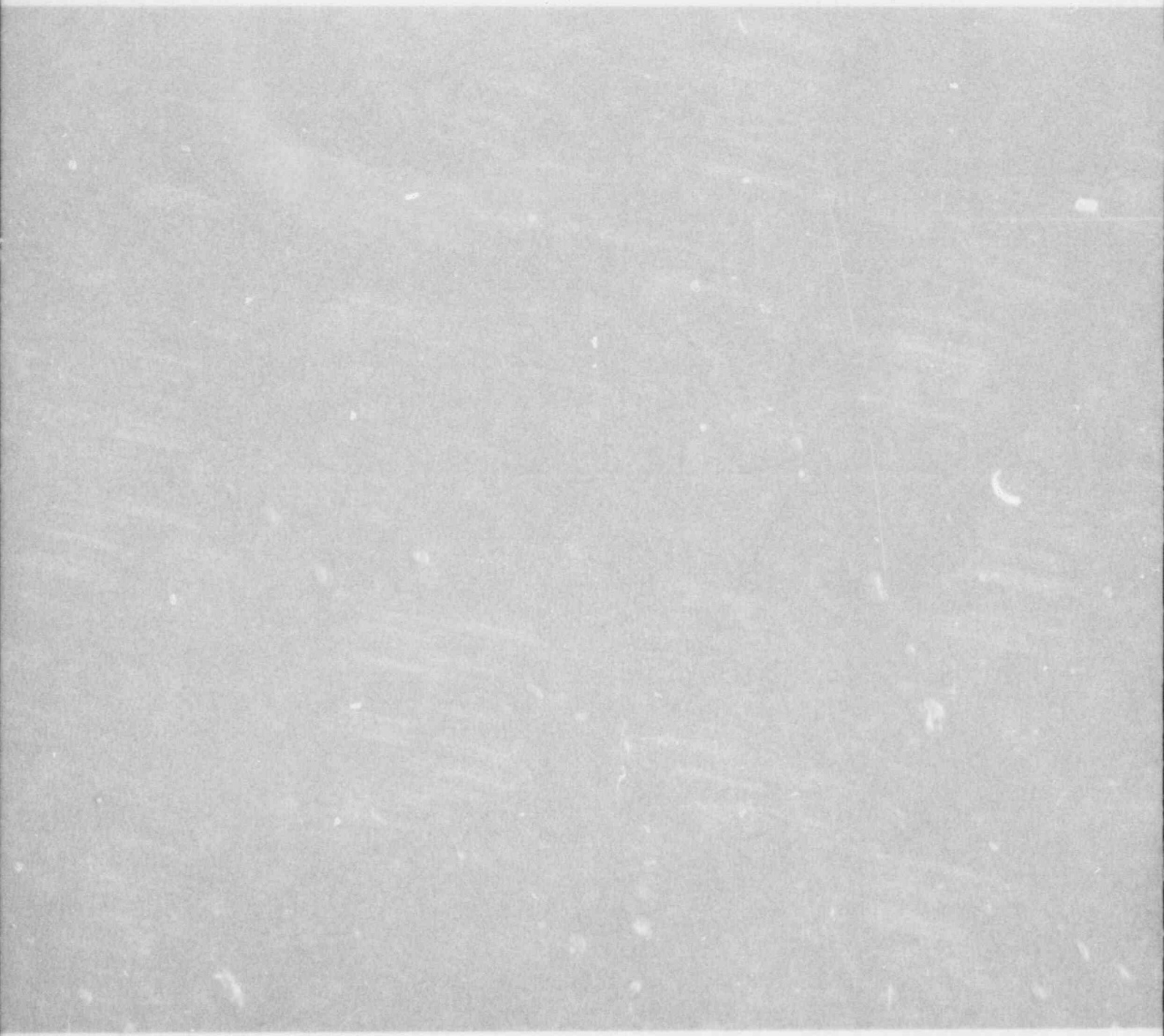

Los Alamos